Azoheteroarene Based Visible Light Photoswitches

Irin P. Tom

A dissertation submitted for the partial fulfilment of

BS-MS dual degree in Science

INDIAN INSTITUTE OF SCIENCE EDUCATION AND RESEARCH MOHALI

April, 2019

To my parents

Mr. Thomas Mathew & Mrs. Marykutty Thomas

Certificate

This is to certify that dissertation titled "**Azoheteroarene Based Visible Light Photoswitches"** submitted by Ms. Irin P. Tom (MS14178) for the partial fulfillment of BS MS dual degree programme of Indian Institute of Science Education and Research Mohali, has been examined by the thesis committee duly appointed by the institute. The committee finds the work done by the candidate satisfactory and recommends that the report be accepted.

Dr. Sugumar Venkataramani	Dr. Sripada S. V. Rama Sastry	Dr. Santanu Kumar Pal
(Supervisor)	(Committee member)	(Committee member)

Dated:

Declaration

The work presented in this dissertation has been carried out by me under the guidance of Dr. Sugumar Venkataramani at the Indian Institute of Science Education and Research Mohali.

This work has not been submitted in part or in full for a degree, a diploma, or a fellowship to any university or institute. Whenever contributions of others are involved, every effort is made to indicate this clearly, with due acknowledgement of collaborative research and discussions. This thesis is a bonafide record of original work done by me and all sources listed within have been detailed in the bibliography.

Irin P. Tom

(candidate)

Dated:

In my capacity as the supervisor of the candidate's project work, I certify that the above statements by the candidate are true to the best of my knowledge.

Dr. Sugumar Venkataramani

(Supervisor)

Acknowledgements

I would like to express my sincere gratitude and thanks to my guide **Dr. Sugumar Venkataramani**, who gave me the wonderful opportunity to join his lab. I thank him for his exemplary guidance, constant supervision and monitoring throughout the course of this work. I thank my committee members Dr. Santanu K. Pal and Dr. S.V. Ramasastry for evaluating my work and giving me valuable suggestions throughout the project. I thank Dr. Santanu K. Pal for being a great mentor also. I express my gratitude towards the current director Dr. Arvind and former directors Prof. DP Sarkar, and Prof. N. Sathamurthy for guiding us. I am thankful to Dr. S. Arulananda Babu, the Head of Department of Chemical Sciences, and Dr. K.S. Viswanathan who was the former Head of Department for all the support they have given me.

I am highly indebted to Ankit K. Gaur and Himanshu Kumar for their supervision and encouragement. I would not ever have been able to complete this project without their help. I acknowledge with a deep sense of gratitude, the cooperation and support received from Physical Organic Chemistry Group, IISER Mohali. I thank Debapriya Gupta for being a great friend. I thank Pravesh Kumar, Surbhi Grewal, Anjali Srivastava, Sonam Suwasia, Mayank Saraswat, Chitranjan Sah, Anjali Mahadevan, Sudha Devi, Amandeep, Amal, Vaitheesh, Virinder, and Divanshu for all their encouragement.

I express my love and thanks toward my parents, sisters and brothers-in-law for always supporting me. I thank Mollykutty teacher, Saly teacher, Graceyamma teacher, Saji sir and Nisha Miss for inspiring me to take research as a career. I am indebted to all my past teachers and friends for all the help and motivation they have given me. Nothing would have been possible without you all.

Finally, I thank DST for the INSPIRE fellowship and Department of Chemistry, IISER Mohali for all the facilities. I also express my gratitude to all other technical and non-technical staff of IISER Mohali.

Irin P. Tom

List of Figures

List of Schemes

List of Tables

Abbreviations

ESI – Electron Spray Ionisation

NMR - Nuclear Magnetic Resonance

ACN- Acetonitrile

MeOH- Methanol

Eq. - Equivalent(s)

AB- Azobenzene

FTIR - Fourier Transform Infrared Spectroscopy

TLC - Thin Layer Chromatography

^{13}C-NMR - Carbon-13 NMR

HOMO- Highest occupied molecular orbital

^{1}H-NMR - Proton NMR

LUMO- Lowest occupied molecular orbital

ATR- Attenuated Total Reflectance

$NaNO_2$ - Sodium nitrite

Contents

Abstract

Azobenzenes are one of the important classes of molecular photoswitches and are widely used in molecular motors, memory, manipulators, solar thermal storage etc. *E*-to *Z*-isomerization of azobenzene happens under UV irradiation. This limits the use of azobenzene as a photoswitch in photobiology as UV light is less penetrating in tissues. To circumvent this issue, attempts have been made to develop visible light photoswitches by introducing Lewis acids, tetra-*ortho*-substitution, ring strain or push pull effects into the photoswitching molecule. Nevertheless, the reported visible light photoswitches suffer from low *Z*-isomer half-life. Since tuning of half-life is equally important as visible light photoswitching, our aim was to combine these two properties and come up with a new genre of photoswithes.

Here, we present a series of visible-light azoheteroarene photoswitches with varying *Z*-isomer lifetimes and good photochemical conversions by using *ortho*-amination. In this regard, we have utilized isoxazoles and N-methylpyrazoles as heterocycles. The advantages of these systems are very long *Z*-isomer half-life apart from visible light photoswitching. Toward this end, 18 *ortho*-substituted azoheteroarenes have been synthesized. Their photoswitching behaviour, solvatochromism, forward and reverse photoisomerization conversion at their respective photostationary states (PSS), and kinetics were investigated and estimated using UV-Vis and NMR spectroscopic techniques.

Chapter 1: Introduction

1.1 Photoswitchable systems

Photoswitches are the molecules that can reversibly undergo changes in structure or properties upon irradiation with light. Examples of photoswitchable systems are azoarenes, stilbenes, spiropyrans, fulgides, diarylethenes, and chromenes. The story of research in the azoarenes started as an answer to the quest for new dyes[1]. By the end of the 19th century, the industrial revolution presented new promises in the textile industry, and a newly found zeal began to appear in the research on dye molecules[2].

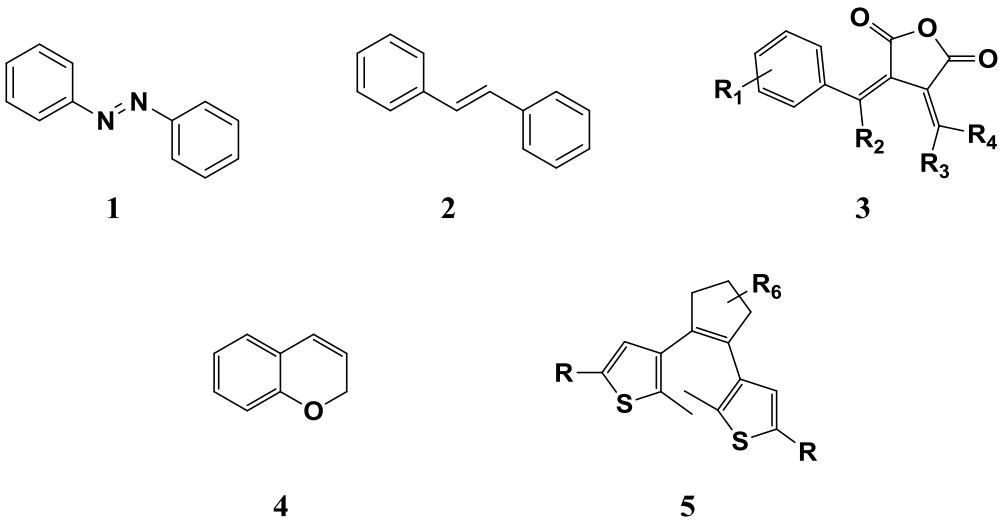

1 **2** **3** **4** **5**

Scheme 1.1 Examples of photoswitches: azoarene (compound **1**), stilbene (compound **2**), fulgide (compound **3**), chromene (compound **5**), diarylethene (compound **6**).

The medicinal activities in various therapeutic areas gave momentum to the studies on azoarene based molecules, in particular, the molecules with heterocyclic moieties[3-6]. Some azoheteroarenes such as Erichrome Black-T, Methyl orange, etc. exhibited pH-induced photochromic behavior and found use as indicators[7,8]. In 1937, Hartley discovered *Z*-isomer of azobenzene (AB) and this established the photoswitching ability of azoarenes[9].

The two isomers of AB vary in their physical properties such as dipole moment, absorption spectral features, planarity, π- conjugation, etc. *Trans* (*E*-isomer) AB adopts a

planar structure with C_{2h} symmetry, whereas *cis* (*Z*-isomer) AB adopts a non-planar conformation with C_2 symmetry.

1.2 Photoisomerization in AB

The azo group exhibit two electronic absorption features namely, π-π* and n-π* bands. In the *E*-isomer, the π-π* absorption is strong, whereas the n-π* absorption is weak. Upon irradiation with UV light, a blue shift occurs in the π-π* band (due to breaking of conjugation) and an enhancement in intensity occurs in n-π* band (due to symmetry allowed transition), revealing the presence of *Z*-isomer. The nature of the bands, as well as the spacing between them, is determined by the substituents[10,11].

Irradiation at a wavelength corresponding to the π- π* band leads to *E*-to *Z*-isomerization (forward switching), whereas irradiation at a wavelength corresponding to the n-π* band leads to *Z*-to *E*-isomerization (reverse switching). If the irradiation is done at a wavelength, which corresponds to the overlapping region of *E*-and *Z*-isomers, both isomerizations can happen simulataneously[10,11]. Various mechanisms including rotation[12], inversion[12], inversion assisted rotation[14] and concerted inversion[13] are proposed for the photoisomerization[11]. The photoisomerization step of azobenzene has always perplexed the researchers owing to the fact that the molecule possesses nitrogen lone pairs. In general, irradiation at wavelengths, which correspond to the π-π* and n-π* bands lead to isomerization through rotation and inversion mechanisms, respectively[15].

In the rotational pathway, the N=N π bond breaks to enable free rotation about the N–N single bond. This changes the C–N–N–C dihedral angle, whereas the N–N–C angle remains fixed around 120^{0} [48]. Inversion pathway involves an increase in one of the N=N–C angles toward 180^{0} while the C–N=N–C dihedral angle remains fixed at 0^{0} leading to a transition state with one sp hybridized azo-nitrogen atom[49]. Notwithstanding large changes in the C–N=N–C dihedral angle, the inversion assisted rotation involves only small changes in the N=N–C angles. The transition state formed in all these three pathways possesses polar transition states in contrary to concerted inversion pathway. In the concerted inversion, both N=N–C bond angles increase (to 180^{0}) and thereby a linear transition state with no net dipole moment is formed[11]. From the four aforementioned

transition states, relaxation can happen to either *Z*-form or *E*-form and this engenders the so-called photostationary states.

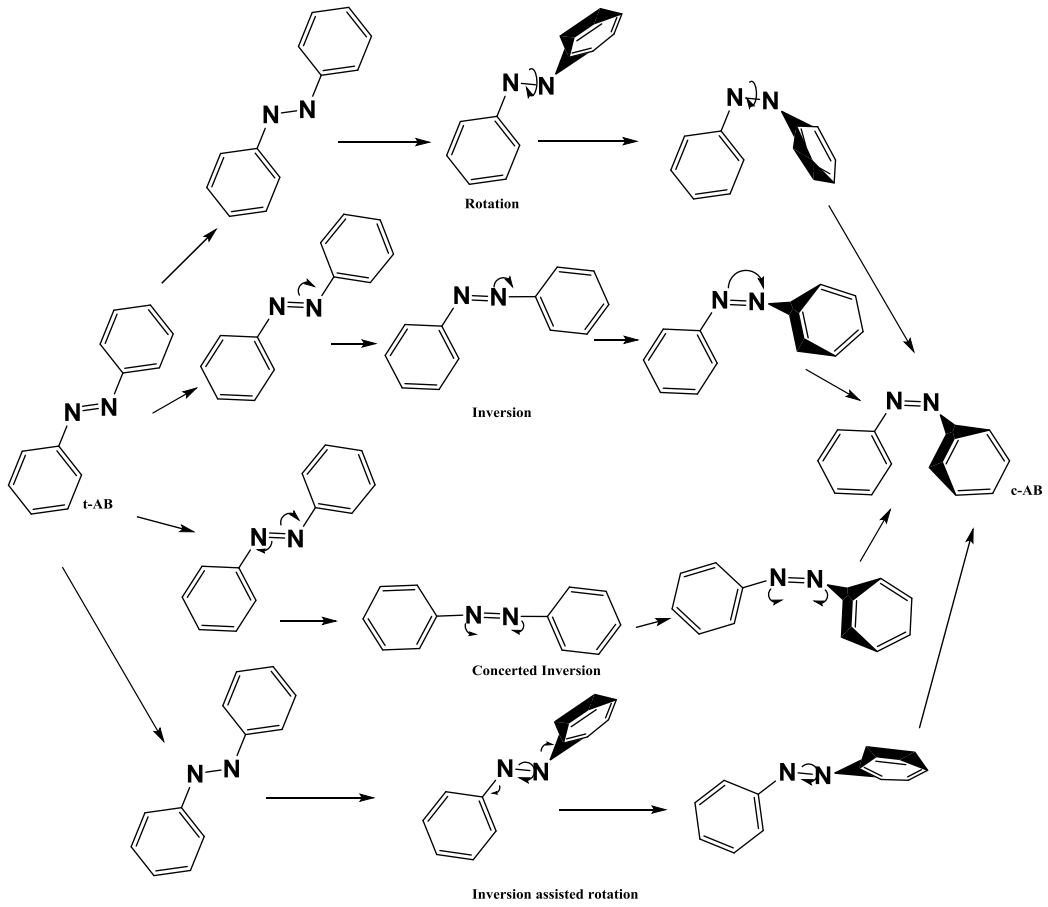

Scheme 1.2 Proposed mechanisms for the *E*- to *Z*-isomerization of AB

In general, photoisomerization phenomena for the azoheteroarenes are investigated using various spectroscopic techniques, especially UV-Vis, NMR and FTIR spectroscopies. These techniques give information regarding the π-π* and n-π* transitions, molar absorption coefficient, PSS estimation, wavelengths corresponding to forward and backward photoswitching, etc. The UV-Vis spectroscopy mainly uses the π-π* and n-π* absorptions of both *E*- and *Z*-isomers whereas the NMR spectroscopic technique utilizes the upfield shifts in the protons (due to shielding effects of the aryl group on the adjacent protons) upon *E*-to *Z*-isomerization. The FTIR spectroscopy uses the shifts and splits of

the peaks arising from the changes in symmetry and geometry of the molecules. Apart from these techniques, femtosecond transient absorption, fluorescence, stimulated Raman spectroscopy and X-ray diffraction techniques have also been used in understanding the *E*-to *Z*-isomerizations[29-32].

1.3 Visible light photoswitchable systems

Push-pull systems are an important class of azoheteroarenes, and these were one of the earlier approaches towards the generation of visible light photoswitches[16,17]. In push-pull systems, electron withdrawing and electron donating parts will be present, thus enabling better π-conjugation which lowers the HOMO-LUMO energy gap. As the HOMO-LUMO gap decreases, the energy corresponding to n-π* absorption decreases, subsequently resulting in a red shift in the n-π* absorption band. Owing to the highly polarized structure, absorption properties of this molecule is highly solvent dependent. The push-pull system based azo dye developed by Santo's group[17] (compound **6**) is given in Scheme 1.1.

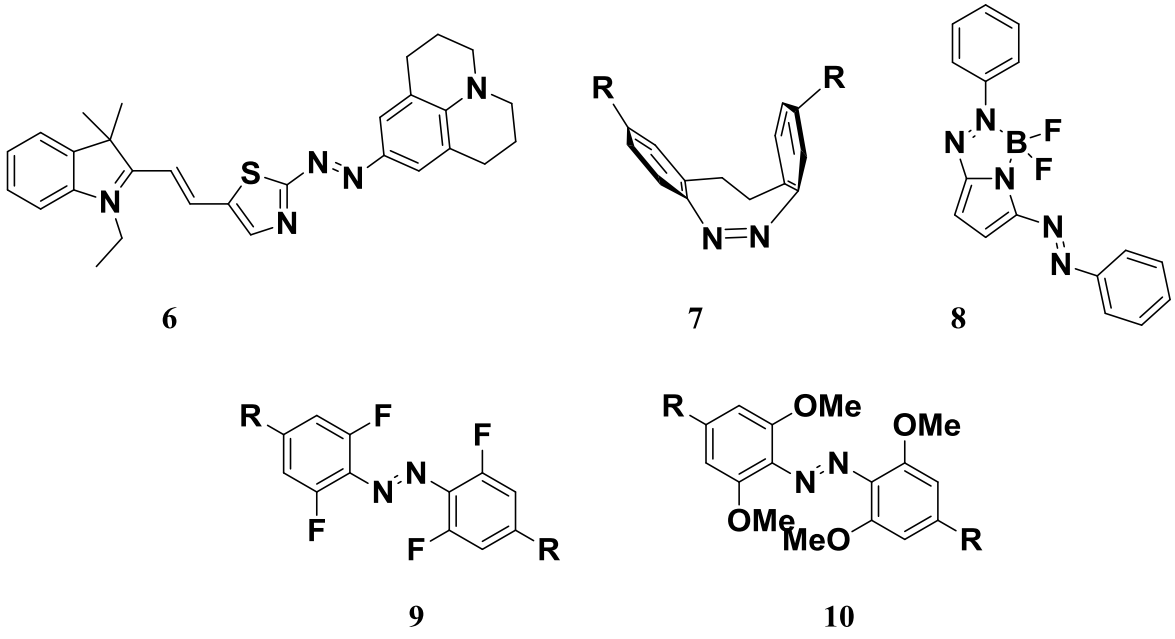

Scheme 1.3 Visible light photoswitches

Based on the kinetic solvent effects, push-pull type substituents containing azoarenes use rotational mechanism[18]. Systems connected to rigid groups like crown ethers utilize inversion mechanism, which can be attributed to restricted molecular motions, enthalpy of solvent transfer and substituent effects [19-21]. Later, Herges and coworkers introduced visible light photoswitches with high ring strain (compound **7** in Scheme 1.3). The ring strain makes *Z*-isomer the thermodynamically stable form at room temperature, in complete contrast to normal ABs[22]

Dolphin and coworkers introduced visible light photoswitches that use Lewis acid (BF_2) coordination (compound **8** in Scheme 1.3)[23]. Relative to normal ABs, binding with BF_2 considerably reduces the energy of n-electrons. On the other hand, additional conjugation in the N-C-C-N-N skeleton makes π-nb (mixing of π- and non-bonding) molecular orbital, high in energy[23]. Aprahamian's group has also come up with BF_2-adducts of ABs, which exhibited exceptional photoswitching characteristics. But, these molecules are converted to hydrazones, and thus their applicability in biological systems is limited[24, 25].

In *ortho*-fluoroazobenzenes, as a consequence of lowering in the energy of the n-orbital through the introduction of *ortho*-fluoro substituents, the Z-isomers of F4-ABs are thermally stable with a half-life of 2 years (compound **9** in Scheme 1.3) in DMSO at 25 ^{0}C[26,27]. Woolley and coworkers introduced tetra-*ortho*-methoxy substituted AB (compound **10** in Scheme 1.3) with two *para*-amido moieties to permit linkage to target biomolecules[28]. In the *E* isomer, π-π* transition was blue-shifted, and the n-π* transition was red-shifted in comparison with the parent compound where there was no methoxy substituents. They attributed this observation to the twisting (non-planarity) of the *E* isomer and interaction of the methoxy groups with the lone pairs of nitrogen on the azo group[28].

A twisted geometry was observed by Fuchter and coworkers for azoheteorarenes with *ortho*-methyl group(s) due to the steric factor which in general, reduces the *Z*-isomer stability[33]. Fast thermal reverse isomerization is exhibited by *Z*-isomers with twisted geometry. The systems which have mono methyl substitution (in the *ortho* position) enjoy two choices, one being the destabilizing twisted geometry and the other option being the stabilizing T-shaped geometry. The energy difference between these two

geometries as well as the barriers relative to them determines the weighted average half-life.

1.4 Tuning of cis-lifetime in photoswitches

Selective control of the *Z*-lifetime of the photoswitches is crucial since preferred switching dynamics vary for different applications. Combining the *Z*-isomer stability and visible light absorption in photoswitches is essential in various fields of research[35] like photobiology. Herges' group has synthesized phenyl azoimidazole derivatives exhibiting a *Z*-isomer half-life of 22 days[34]. This improvement must be seen in the light of AB *Z*-isomer half-life, which is 4 hrs. In the *Z*-aryl azoimidazole, the imidazole ring is coplanar with C–N═N–C plane, and the phenyl ring is orthogonal with respect to the plane, which prevents conjugation between the two rings[34]. This is opposite to the case of AB where both phenyl rings are twisted out of planarity by about 56^0 with respect to the C–N═N–C plane in the Z-isomer[36]. The π-π* absorptions are well separated in both isomers since there is a huge difference in conjugation. *E*-isomer exhibits a strong absorption band at 365 nm compared to the *Z*-form. This has been suggested as the reason behind the efficient reverse switching of this genre of molecules. Since the π-π* transitions in the azoimidazoles partially overlap with the n-π* transitions, the photochemical back switching, which is usually performed with visible light of approximately 450 nm in ABs and azopyridines is found to be inefficient in the azoimidazoles[34].

Later, Fuchter and coworkers introduced aryl azopyrazoles, a class of azoheteroarenes, which exhibit a *Z*-isomer half-life reaching up to 1000 days[37]. Bidirectional photoswitching is enabled in this class of molecules due to the large separation of the λ_{max} values of the *E*-and *Z*-isomers. The five-membered aromatic rings, in contrast to the six-membered aromatic rings of AB, holds many implications as it allows the *Z*-forms of these azoheteroarenes to adopt a conformational geometry, which is not accessible to AB derivatives[37]. Additional steric tuning can be imposed on these molecules by substitution on the heterocyclic ring and this has a major effect on the n-π* absorption. The Z-isomers of this family of molecules can adopt a conformation where heteroarene and azo group are coplanar and approximately orthogonal to the phenyl ring, in contrast to the azobenzene case where such a conformation is impractical because of the large ring size.

This can reduce the intensity of the n-π* absorption of the *Z*-isomer. Selective tuning can be made using the substituents on the heteroaromatic ring as they can induce steric effects to a varying degree[37].

However, the use of intense irradiation is not pragmatic in photobiological applications because penetration of UV light is less in tissues. Also, the UV light has damaging effects on tissues. To circumvent this issue, researchers have been utilizing photoswitches with photosensitizers such as two-photon fluorophores[38], triplet sensitizers[39,41] and upconverting nanophosphors[40]. These molecules will transfer the collected excitation energy from radiation absorbed in the visible or near-infrared (NIR) region to the molecular photoswitches via Förster resonance energy transfer (FRET), TTA, or simply by UV emission/re-absorption, thus helping their isomerization. These approaches need to use sensitizers along with photoswitches. Ethylene-bridged azobenzene synthesized by Herges bypasses this trouble[42]. Due to the ring strain in this molecule, *Z*- rather than the *E*-form is the thermodynamically stable form at room temperature (in complete contrast to normal ABs). Also, the n-π* absorption of the *E*-isomer is stronger than that of the *Z*-isomer. Hence, photoswitching of this molecule can be done making use of well-resolved n-π* absorption bands of *E*-and *Z*-form. Tetra- *ortho*-methoxy AB synthesized by Woolley also overcomes this difficulty[28, 43-44]. The separation of the n-π* bands of *E*- and *Z*-isomers of these molecules enable *E*-to-*Z*-isomerization to happen in green light (at wavelengths, which correspond to the excitation in the n-π* band of the *E*-isomer). This is in stark contrast with the case of unsubstituted AB where irradiation at wavelengths, which correspond to the n-π* band leads to reverse photoswitching. The repulsive interactions between lone pairs of the oxygen and nitrogen atoms destabilize the n-orbital of *Z*-isomer of AB.

Ortho-fluorination of the azobenzene can induce better stability for *Z*-isomer. Hecht's group came up with bidirectional photoswitching through *ortho*-fluorination[45]. Introducing σ-electron withdrawing fluorine atoms *ortho* to the N=N unit results in fast visible light photoisomerization with high photoconversion rate[45]. It also offers the realization of a bistable photoswitch. The increased *Z*-isomer lifetime promised by this class of ABs is a reflection of the reduced electronic repulsion in their HOMOs. Large

dihedral angle around the N-C single bond reduces the π-electron delocalization in the *Z*-AB leading towards a π*-orbital, which is raised in energy. The n-orbital of *Z*-AB is higher in energy compared to the n orbital of *E*-AB. The lone pair orbitals in *Z*-isomer interact through space and engender two MOs, whose higher energy MO serves as the HOMO, whereas the n orbital of *E*-AB is equivalent to a linear combination of lone pair electrons of the two N atoms. The lone pair interaction here is taking place via mixing with the σ-bonding orbital[46] and the antibonding combination here acts similar to the n-orbital. So, the introduction of σ-electron withdrawing group resulted in the separation of the n-π* bands of the *E*- and *Z*-isomers[45]. Additional electron withdrawing groups in the *para*-position further increase the separation of n-π* transitions of *E*-and *Z*-isomers[45]. The drawback associated with *ortho*-fluorinated ABs is their low molar absorptivities in the visible region.

Woolley and coworkers have introduced *ortho*-amination for enhanced molar absorptivity in the visible range[47]. The problem underlying this method is the decrease in *Z*-isomer lifetime. *Ortho*-Methoxylation can increase both *Z*-isomer lifetime as well as the molar absorption coefficient although the increase in the latter is only moderate[28].

1.5 Motivation and Design

Our aim was to create a new genre of molecular photoswitches where visible light photoswitching and tunability of *Z*-isomer lifetime are combined. We decided to choose *ortho*-amination in order to induce visible light photoswitching in the photoswitches. The emergence and also the increasing popularity of azoheteroarene based photoswitches and their inherently better *Z*-isomer lifetime motivated us to concentrate on azoheteroarene based visible light photoswitches. To study the effect of the ring size and nature of the amine on photoswitching wavelength, we decided to use pyrrolidine, piperidine, azepane, morpholine and piperazine substitution. To study the nature of heterocycle in determining the *Z*-isomer lifetime of the molecules, we designed molecules belonging to different classes of heterocycles namely isoxazole and N-methylpyrazole.

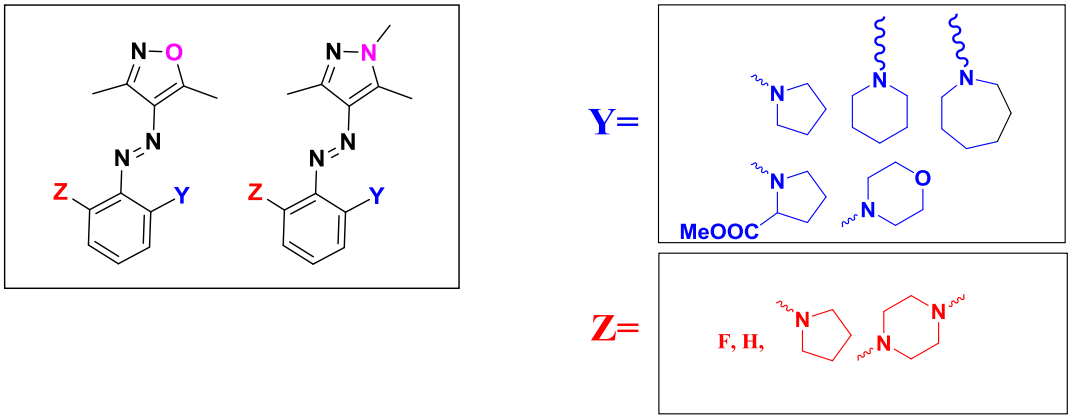

Scheme 1.4 Target design

Chapter 2: Results and Discussion

2.1 Synthesis

Azo group can activate vicinal halogens toward nucleophilic aromatic substitution in *ortho*-halogenated azobenzenes[51,52] and fluoride is considered to be an excellent leaving group in an aromatic system. Combining these two factors, Priimagi and coworkers introduced a scheme[50] for *ortho*-amino substituted AB where the amino groups are conveniently introduced by replacing *ortho*-fluorines in *ortho*-fluoroazobenzenes[45]. We followed the same synthetic strategy for the synthesis of our molecules. Scheme 2.1 shows the optimized reaction scheme. A library of molecules that we made is given in the scheme with their respective yields. All the synthesized molecules have been fully characterized by ^{1}H, ^{13}C-NMR, HRMS, IR, and UV-Vis spectroscopic techniques. Mainly two different heterocycles namely, 3,5-dimethyl isoxazole and 1,3,5-trimethyl pyrazole have been utilized as heterocycles for the azoheteroarene part.

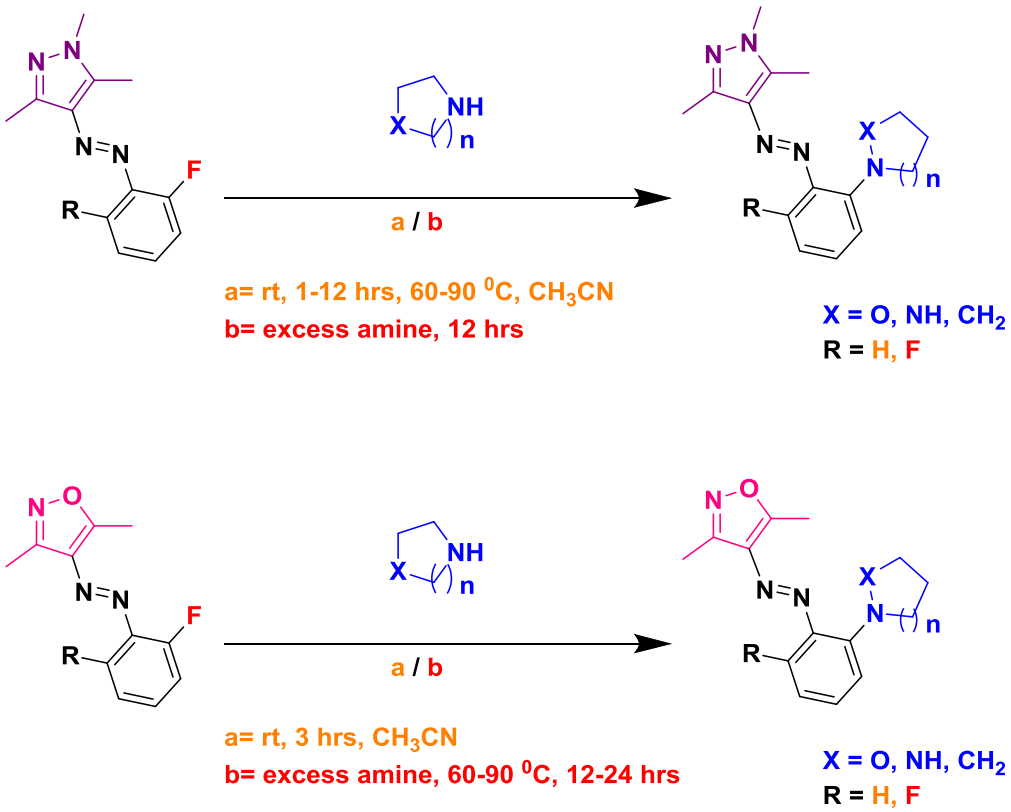

Scheme 2.1 General scheme for reactions

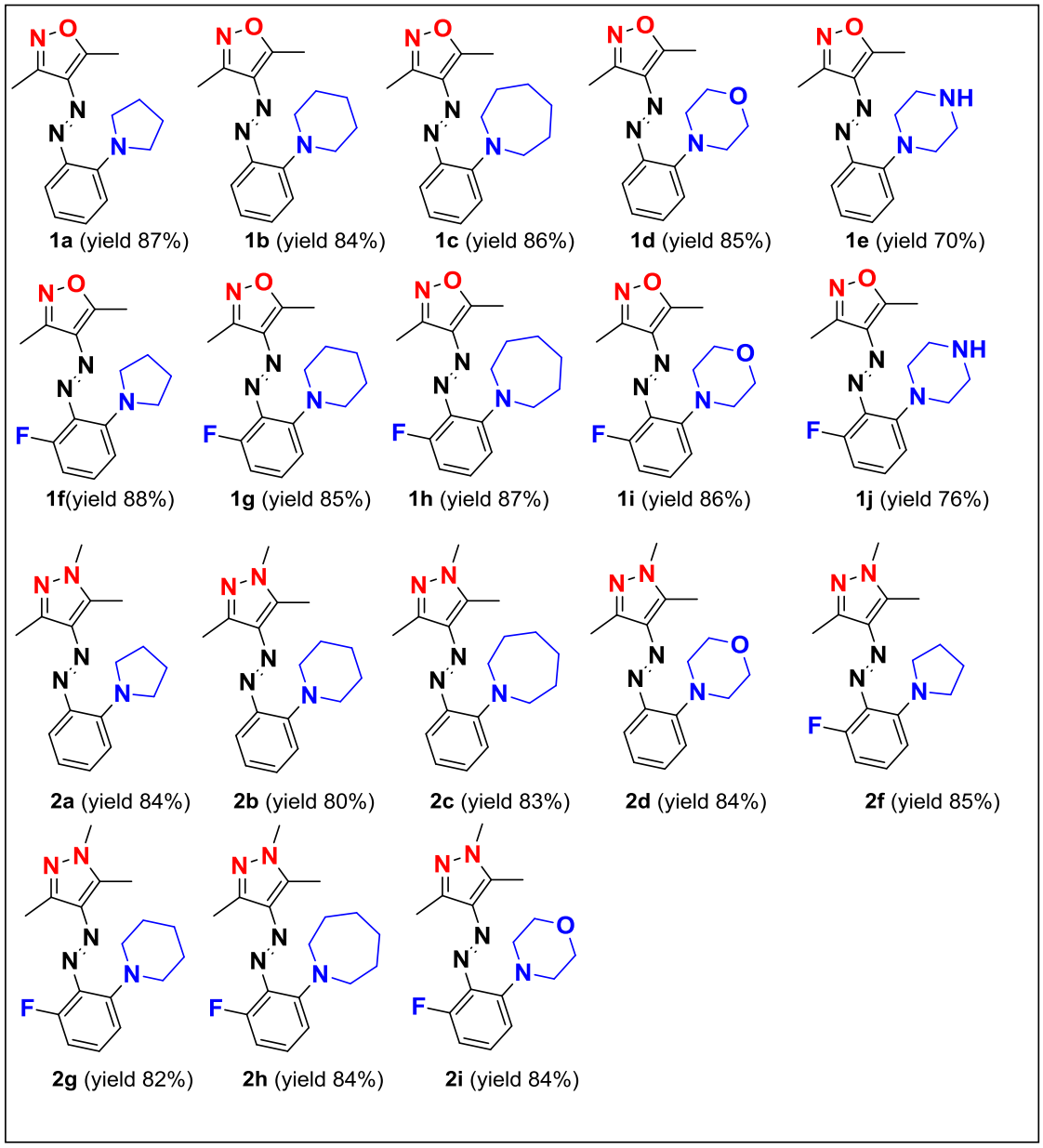

Scheme 2.2 Photoswitches with their respective yields

2.2 Analysis of photoswitching using UV-Vis spectroscopy

The UV-Vis absorption spectra of the all the azoheteroarenes have been measured in CH_3CN. First, the absorbance spectrum was recorded after heating in order to ensure that the molecules are in their thermodynamically stable state (*E*-isomer). Then, the

compounds were irradiated at various wavelengths of light to identify the appropriate wavelength, at which switching (isomerization) can be maximum. The UV-Vis absorption of the compound was recorded at its PSS (photostationary state). A different wavelength of light was used to induce the *Z*-to *E*-(reverse) isomerization.

Table. 2.1 UV-Vis absorption data

Sl. No.	**Compound**	***E* isomer[a]**					***Z* isomer[a]**			**PSS 1[b] (%*E*-*Z*)**	**PSS 2[c] (%*Z*-*E*)**
		λ_1	**ε**	**λ_2**	**λ_3**	**ε**	**λ_1**	**λ_2**	**λ_3**		
1	**1a**	310	9576	415	470	7586	392	_	474	28	16
2.	**1b**	315	14919	406	458	5302	309	382	438	66	10
3.	**1c**	314	-	408	465	11330	307	397	468	19	4
4.	**1d**	313	10386	397	447	4157	310	385	442	56	35
5.	**1e**	318	5430	405	443	2026	_	_	435	63	21
6.	**1f**	313	7701	384	436	2597	300	357	441	37	29
7.	**1g**	306	5639	384	445	2141	305	368	437	60	15
8.	**1h**	314	7345	408	447	1413	302	_	450	57	25
9.	**1i**	309	6074	400	450	3359	300	_	445	61	17
10.	**1j**	309	11660	384	443	7701	306	354	436	62	14
11.	**2a**	324	5457	407	448	3612	_	402	444	46	42
12.	**2f**	318	12382	_	449	3832	315	_	453	21	12

The photoswitching studies were primarily conducted in CH_3CN, however, for selected candidates solvents like DMSO and MeOH were also used in order to check whether the molecules were exhibiting solvatochromism. We have carried out photoswitching with *ortho*-amino substituted isoxazole and pyrazole derivatives. The spectra of each compound before irradiation as well as at photostationary states (PSS) corresponding to forward switching and reverse switching are shown in Appendix 5C, and the corresponding spectroscopic data including isomerization rate are summarized in Table. 2.1.

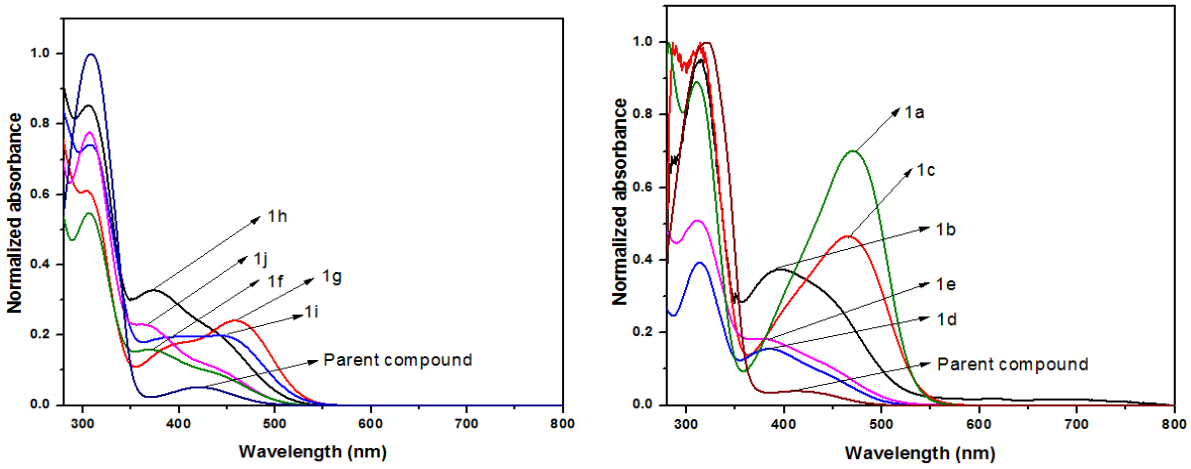

(a) (b)

Fig. 2.1 Comparison of UV-Vis absorption spectrum of compounds in CH_3CN solvent

The switching wavelength required by our molecules range from 405 to 490 nm. The comparison of UV-Vis absorption spectra of compounds **1a**-**1e** with their parent molecule ((*E*)-4-((2-fluorophenyl)diazenyl)-3,5-dimethylisoxazole) is given in Fig. 2.1 (a), whereas the comparison of UV-Vis absorption spectra of compounds **1f**-**1j** with their parent molecule ((*E*)-4-((2,6-difluorophenyl)diazenyl)-3,5-dimethylisoxazole) is given in Fig. 2.1 (b). The spectral properties undergo noticeable change under *ortho*-substitution.

We noticed the splitting of n-π* absorption band in the UV-Vis absorption spectra of our molecules. In normal ABs, the n-orbitals of both nitrogen atoms are degenerate, whereas

this degeneracy is lost in our molecules, presumably the lack of symmetry on both sides of the azo bond could be reason for it. Now, these newly emerged strongly absorbing bands can effectively be utilized for photoswitching using visible light.

The molecules with pyrrolidine substitution at *ortho* position showed a maximum red shift in the absorption spectra compared to azepane and piperidine substitutions. The plausible reasons for the red shift can be the conformations of the cyclic amines connected to phenyl group and also the interaction between azo nitrogen and C-H of the amine. Wolley and coworkers reported that among various factors steric reasons could be pointed out as a cause of the variation in the hybridization of nitrogen atom that caused the observed red shift[47]. In this regard, the five-membered (pyrrolidine) was found to have more sp^2 hybridization character than the six-membered (piperidine) ring system. Based on this report, we hypothesize that either a folded envelope or twisted conformation of pyrrolidine has greater delocalization of electron density from nitrogen lone pair to aryl ring than the chair conformation of the six membered rings. Otherwise, an additional C-H-N(azo) contact may stabilize the sp^2 hybridization of five-membered ring than in the six-membered ring system. As the delocalization increases, the HOMO-LUMO gap decreases resulting in a red shift of the n-π* band. The conformations of azepane near the azo group may be similar to that of pyrrolidine, enabling it to exhibit a better red shift in the n-π* band compared to piperidine. When there is a heteroatom like oxygen or nitrogen present in the piperidine ring, the basicity of the amine is expected to be less as the heteroatom will be trying to pull electron density towards it, and this was evident in the absorption spectra obtained in the case of morpholine and piperazine substitutions[47].

Kinetic studies have been carried out for selected molecules. The kinetic plot obtained for compound **1a** is given in Fig. 2.2. Since the reverse isomerization is following first order kinetcs, half-life of Z-isomer can be estimated through kinetic studies. The half-lives obtained for pyrrolidine substituted photoswitches we synthesized range from minutes to days. Long-term photoswitching studies have also been carried out for selected molecules. The long-term studies using compound **1a** in CH_3CN shows stability upto 5 cycles (Fig. 2.3).

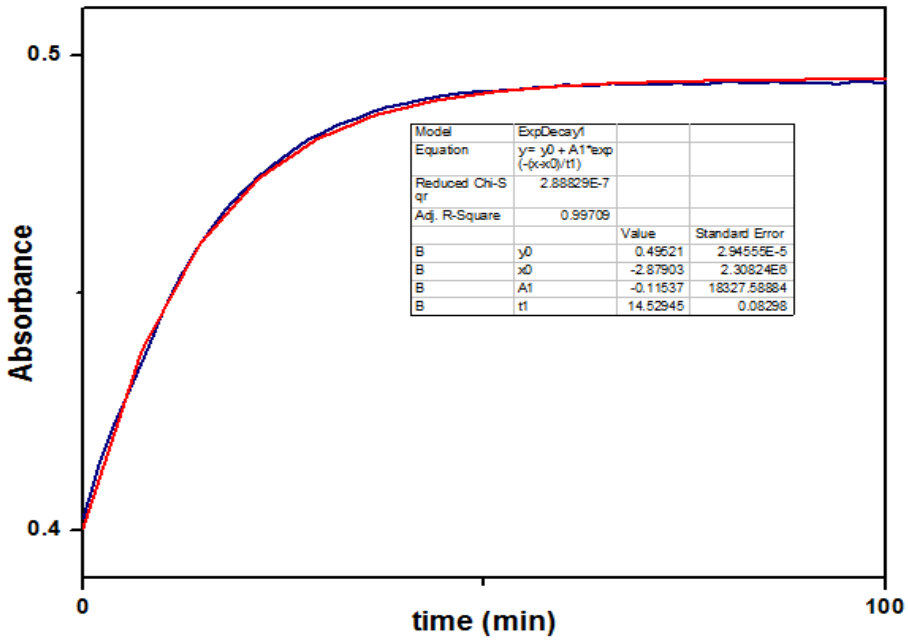

Fig. 2.2 Kinetic plot of compound **1a**

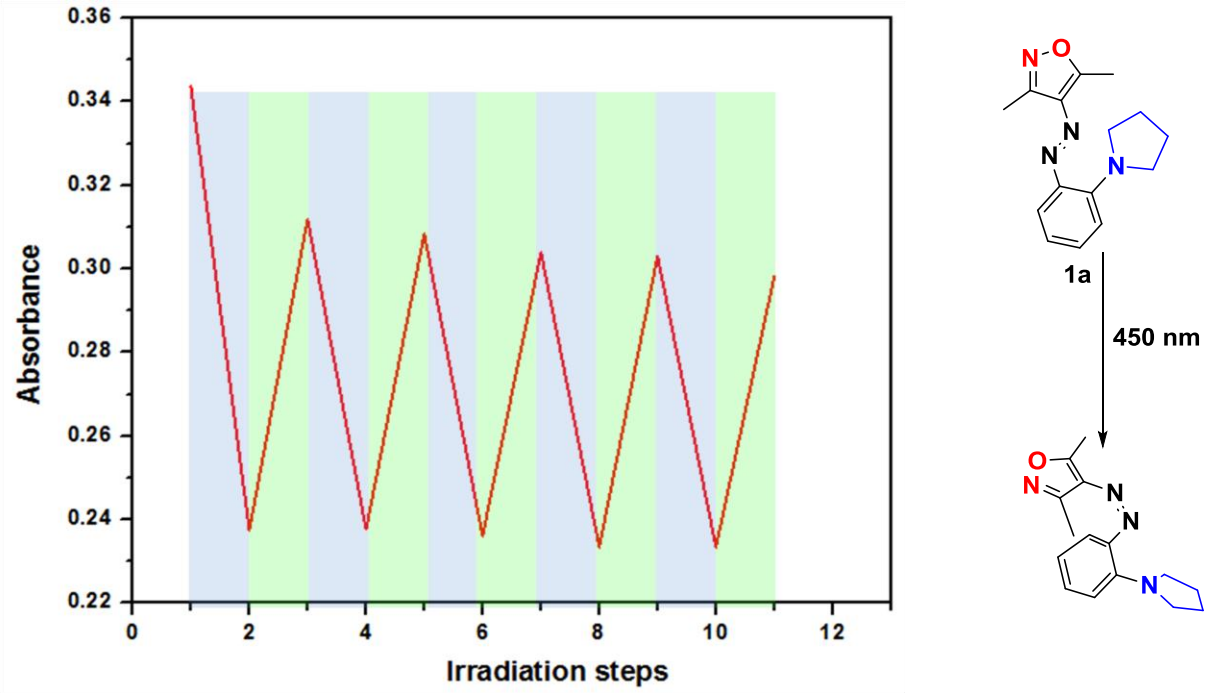

Fig. 2.3 Long-term photoswitching of compound **1a** (Forward switching: 450 nm; Reverse isomerization: 535 nm)

2.3 Analysis of photoswitching using NMR spectroscopy

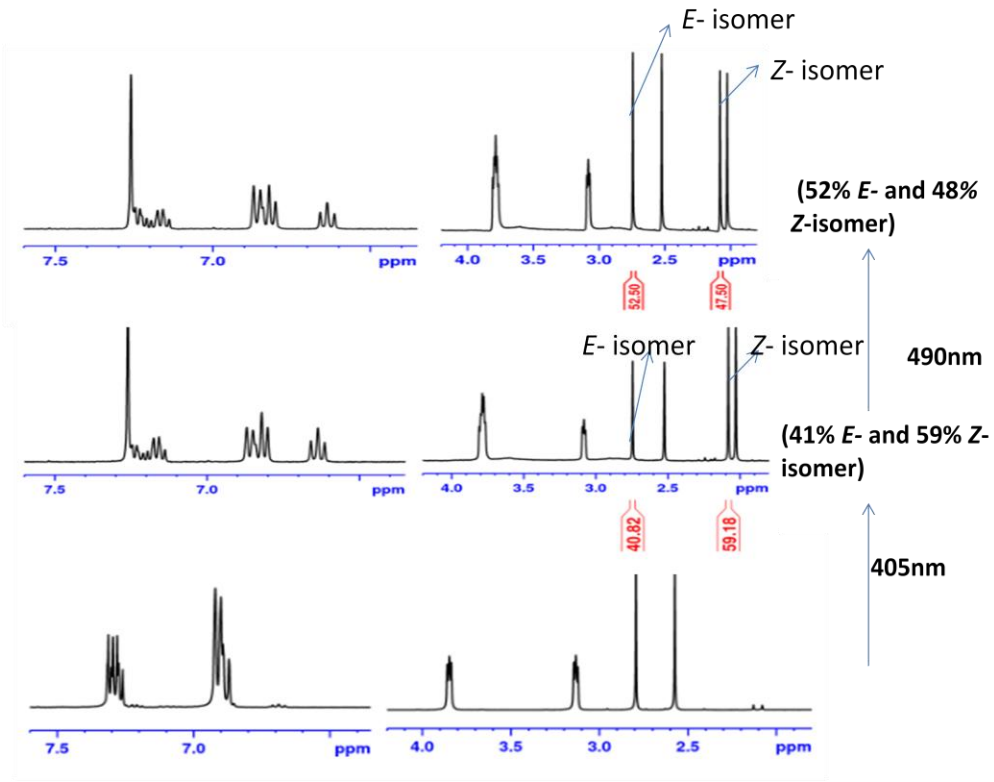

Fig. 2.4 NMR photoswitching of compound **2i** in $CDCl_3$

NMR photoswitching studies have been carried out in $CDCl_3$ solvent. Fig. 2.4 depicts the nmr photoswitching of compound **2i**. Before photoswitching, molecules showed the proton signals corresponding to *E*-isomer. Upon irradiation at 405 nm, *E*-*Z* isomerization took place and shielding of proton signals occur because of the ring current. Fig.2.4 depicts that the conversion for *E* to *Z* photoisomerization of compound **2i** is upto 59% and the reverse *Z*- to *E*-isomerization is upto 52%. The nmr photoswitching data for the selected molecules are given in Appendix 5D.

Chapter 3: Summary and outlook

3.1 Summary

In the near future, research in visible light photoswitches will be accelerated as researchers have shown that the use of photoswitches in photobiological systems offer a wide range of possibilities. AB has become a holy grail for the scientific community owing to its multifaceted properties and simplicity as a molecular switch. Compared to AB, azoheteroarene molecules are less investigated as photoswitches. The goal of our project was to develop a new genre of visible light photoswitches with tunability in *Z*-isomer lifetime. In this regard, we successfully synthesized 18 azoheteroarene molecules in good to excellent yields.

All the molecules with pyrrolidine substitution at the *ortho*-position showed more red shift in absorption maxima compared to the piperidine substitution. The nitrogen atom will be sp^2 hybridized in the pyrrolidine ring. On the other hand, the sp^2 character of nitogen atom will be less in piperidine ring as its chair conformation is sterically hindered. Also, there is a possibility of an additional C-H-N(azo) contact in pyrrolidine. Close to the azo bond, azepane has a conformation that has a resemblance to the pyrrolidine ring and hence it possesses better capacity for electron delocalization compared to the six-membered cyclic amines. Also, it was observed that the red shift in the absorption wavelength was less in the cases, where there was a heteroatom in the 2′ position in the pipiridine ring. As a heteroatom which is more electronegative than C atom is present at the 2′ position, the basicity of the amine N will be reduced.

We observed the splitting of the n-π* band in the UV-Vis absorption spectra of our molecules and this might be caused by the loss of degeneracy of n-orbitals of nitrogen atoms of the azo group. Kinetic studies carried out on our molecules reveal that our molecules possess tunability in *Z*-isomer half-life. The long-term photoswitching studies carried out on selected molecules provide a glimpse into the excellent stability of our photoswitches.

One limitation we encountered is in the recording of ^{13}C NMR spectrum. Heating the compound before recording can prevent the appearance of *Z*-isomer signals in ^{1}H NMR.

The recording of ^{13}C NMR spectra takes much more time than ^{1}H NMR spectra. Due to this reason, the presence of *Z*-isomer is common in the ^{13}C NMR spectra of our molecules.

3.2 Outlook

Light can be used with good spatio-temporal precision in biological systems. Photoswitches can be used to create cages for functional molecules. Photoswitchable cages make it possible even to remove the functional molecule after a particular aim is accomplished. Another advantage of photoswitchable molecules is their ability to bind with proteins and DNA molecules. As the switching happens in the photoswitch, conformation of the biomolecule will subsequently undergo changes. Our ultimate aim is to develop molecules which can be used in photobiological applications either *ex vivo* or *in vivo*.

UV-Vis kinetic studies of our molecules are under progress. We plan to extend our substrate scope and carry out NMR Kinetic studies, and pH studies for selected molecules.

Chapter 4: Materials and methods

4.1 General

All commercially available reagents and solvents were purchased either from Sigma Aldrich, TCI, Alfa Aesar or Avra and were used without further purifications unless otherwise mentioned. Purification of the products was carried out either by column chromatography on Silica gel (Merck) mesh size 100-200µm or on neutral alumina. Thin layer chromatography was performed on Merck Silica gel 60 F254 TLC plates. ^{1}H and ^{13}C NMR spectra were recorded in $CDCl_3$ (Sigma Aldrich) in Bruker Avance-III 400 MHz spectrometer (operation frequencies 400 MHz and 100 MHz, respectively). Chemical shift (δ) values are reported in parts per million (ppm) and Coupling constants (J) are reported in Hz. Signals of residual $CDCl_3$ (7.26 ppm) has been used for internal calibration. High resolution mass spectra have been recorded using Waters Synapt G2-Si Q-TOF mass spectrometer. HRMS spectra were obtained from a TOF mass analyser using electrospray ionization (ESI) in both positive and negative modes. FT-IR spectra were recorded on a Perkin-Elmer ATR spectrometer. UV-Vis photoswitching (both solution and solid state) and kinetics studies have been performed using quartz cuvettes on an Agilent Cary 5000 UV-Vis NIR spectrophotometer, whereas the corresponding NMR experiments have been performed in Bruker Avance-III 400 MHz spectrometer. Photoexcitation experiments were conducted using commercial 365nm laser light source or commercial LED light source from Applied Photophysics.

4.2 Synthesis

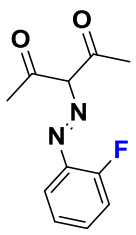

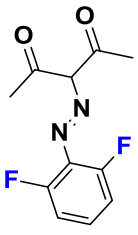

A solution of 2,6-difluoroanline or 2-fluoroaniline (36 mmol) in water (8 mL) was cooled to 0 ^{0}C. To this 37% conc. HCl (8 mL) was added and stirred to get a clear solution. Then

a cold aqueous solution of sodium nitrite (43 mmol in 5 mL of water) was added dropwise into the reaction mixture. After the addition, diazonium salt formation was visible. The reaction mixture was allowed to stir for half an hour for completion. Afterwards, at 0 ^{0}C, a cold aqueous solution of sodium acetate (256 mmol) and acetyl acetone (3.84 mL, 38 mmol) in 30 mL of water was added. The reaction was continued at RT and was monitored by TLC. After completion of the reaction, the reaction mixture was filtered off to obtain a yellow-orange solid product, which was dried under vacuum to yield the desired product.

Synthesis of (*E*)-4-((2-fluorophenyl)diazenyl)-3,5-dimethylisoxazole:

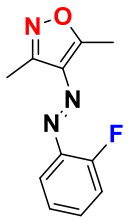

A mixture of (*E*)-3-((2-fluorophenyl)diazenyl)pentane-2,4-dione (2.0 g, 9.0 mmol), Hydrazine Hydrochloride (1.24 g, 18.0 mmol) and Na_2CO_3 (3.81g, 36.0 mmol) in Methanol (60 mL) was refluxed at 72 ^{0}C for 12 hrs. The reaction was followed using TLC up to the completion of the reaction. After completion of the reaction, the product was purified by column chromatography. (Eluent: 5% ethylacetate/n-hexane)

Synthesis of (*E*)-4-((2,6-difluorophenyl)diazenyl)-3,5-dimethylisoxazole:

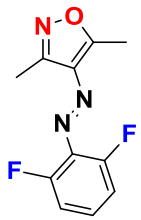

A mixture of (*E*)-3-((2,6-difluorophenyl)diazenyl)pentane-2,4-dione (2.1 g, 9.0 mmol), Hydrazine Hydrochloride (1.24 g, 18.0 mmol) and Na_2CO_3 (3.81g, 36.0 mmol) in Methanol (60 mL) was refluxed at 72 ^{0}C for 12 hrs. The reaction was followed using

TLC up to the completion of the reaction. After completion of the reaction, the product was purified by column chromatography. (Eluent: 5% ethylacetate/n-hexane)

Synthesis of (*E*)-4-((2-fluorophenyl)diazenyl)-3,5-dimethylpyrazole:

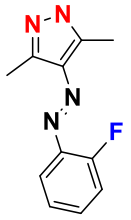

A mixture of (*E*)-3-((2-fluorophenyl)diazenyl)pentane-2,4-dione (2.0 g, 9.0 mmol)), Methylhydrazine sulfate (3.1 g, 21.6 mmol) and Na_2CO_3 (3.81g, 36.0 mmol) in Methanol (60 mL) was refluxed at 72 ^{0}C for 12 hrs. The reaction was followed using TLC up to the completion of the reaction. After completion of the reaction, the product was purified by column chromatography.

Synthesis of (*E*)-4-((2,6-difluorophenyl)diazenyl)-3,5-dimethylpyrazole:

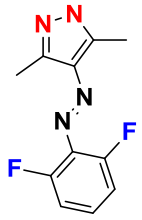

A mixture of (*E*)-3-((2,6-difluorophenyl)diazenyl)pentane-2,4-dione (2.1 g, 9.0 mmol), Methylhydrazine sulfate (3.1 g, 21.6 mmol) and Na_2CO_3 (3.81g, 36.0 mmol) in Methanol (60 mL) was refluxed at 72 ^{0}C for 12 hrs. The reaction was followed using TLC up to the completion of the reaction. After completion of the reaction, the product was purified by column chromatography.

(*E*)-4-((2-fluoro-6-(pyrrolidin-1-yl)phenyl)diazenyl)-3,5-dimethylisoxazole

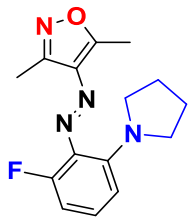

A mixture of (*E*)-4-((2,6-difluorophenyl)diazenyl)-3,5-dimethylisoxazole (50 mg, 0.2 mmol) and pyrrolidine (80 µL, 1 mmol) in MeCN (2 mL) was stirred at room temperature for 3 hrs. The reaction mixture was washed with ethyl acetate and concentrated on rotary evaporator. The crude was purified by column chromatography on silica gel using distilled hexane to yield the product (51 mg, 0.18 mmol, 88%) as orange-yellow solid.

(*E*)-3,5-dimethyl-4-((2-(pyrrolidin-1-yl)phenyl)diazenyl)isoxazole

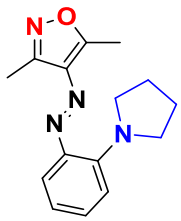

A mixture of (*E*)-4-((2-fluorophenyl)diazenyl)-3,5-dimethylisoxazole (50mg, 0.2 mmol) in pyrrolidine (4 mL) was stirred overnight at 60 ^{o}C. The reaction mixture was washed with ethyl acetate and concentrated on rotary evaporator. The crude was purified by column chromatography on silica gel using distilled hexane to yield the product (47mg, 0.17mmol, 87%) as orange-yellow solid.

Color: orange, ^{1}H NMR (400MHz, $CDCl_3$) δ 1.95-1.99 (t, J= 16Hz, 4H), 2.47 (s, 3H), 2.69 (s, 3H), 3.54-3.57 (m, J= 12Hz, 4H), 6.66-6.70 (m, J= 12Hz, 1H), 6.81-6.83 (m, J= 8Hz, 1H), 7.23-7.27 (m, J= 16Hz, 1H), 7.52-7.54 (d, J= 8Hz, 1H); **HRMS-ESI**: m/z $[M+H]^{+}$: 271.1568.

(*E*)-4-((2-fluoro-6-(piperidin-1-yl)phenyl)diazenyl)-3,5-dimethylisoxazole

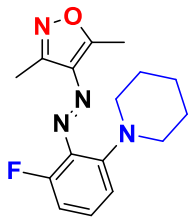

A mixture of (E)-4-((2,6-difluorophenyl)diazenyl)-3,5-dimethylisoxazole (50 mg, 0.2 mmol) and piperidine (99 µL, 1 mmol) in MeCN (2 mL) was stirred at room temperature for 3 hrs. The reaction mixture was washed with ethyl acetate and concentrated on rotary evaporator. The crude was purified by column chromatography on silica gel using distilled hexane to yield the product (51 mg, 0.17mmol, 85%) as orange solid.

Color: orange, **^{1}H NMR** (400MHz, $CDCl_3$) δ 1.53-1.57 (m, J= 16Hz, 2H), 1.62-1.66 (m, J= 16Hz, 4H), 2.54 (s, 3H), 2.74 (s, 3H), 3.01-3.05 (t, J= 16Hz, 4H), 6.74-6.78 (m, J= 16Hz, 1H), 6.83-6.86 (m, J= 12Hz, 1H), 7.13-7.20 (d of d, J= 28Hz, 1H); **HRMS-ESI**: m/z $[M+H]^+$: 303.1563.

IR (ATR, cm^{-1}): 725, 783, 992, 1241, 1410, 1449, 1595, 2806, 2853, 2935.

(*E*)-3,5-dimethyl-4-((2-(piperidin-1-yl)phenyl)diazenyl)isoxazole

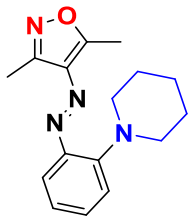

A mixture of (*E*)-4-((2-fluorophenyl)diazenyl)-3,5-dimethylisoxazole (50 mg, 0.2 mmol) in piperidine (4 mL) was stirred overnight at 60 ^oC. The reaction mixture was washed with ethyl acetate and concentrated on rotary evaporator. The crude was purified by column chromatography on silica gel using distilled hexane to yield the product (48 mg, 0.17mmol, 84%) as orange solid.

Color: orange, ^{1}H NMR (400MHz, $CDCl_3$) δ 1.58-1.62 (m, J= 16Hz, 2H), 1.74-1.76 (m, J= 8Hz, 4H), 2.58 (s, 3H), 2.77 (s, 3H), 3.84 (t, J=, 4H), 6.97-7.01 (m, J= 16Hz, 1H), 7.10-7.12 (d, J= 8Hz, 1H), 7.33-7.37 (m, J= 16Hz, 1H), 7.51-7.53 (d, J= 8Hz, 1H).

IR (ATR, cm^{-1}): 755, 912, 923, 1048, 1126, 1227, 1279, 1336, 1385, 1411, 1442, 1481, 1589, 2820, 2854, 2934.

(*E*)-4-((2-(azepan-1-yl)-6-fluorophenyl)diazenyl)-3,5-dimethylisoxazole

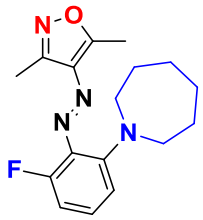

A mixture of (*E*)-4-((2,6-difluorophenyl)diazenyl)-3,5-dimethylisoxazole (50 mg, 0.2 mmol) and azepane (113 µL, 1 mmol) in MeCN (2 mL) was stirred at room temperature for 3 hrs. The reaction mixture was washed with ethyl acetate and concentrated on rotary evaporator. The crude was purified by column chromatography on silica gel using distilled hexane to yield the product (55 mg, 0.17mmol, 87%) as orange solid.

(*E*)-4-((2-(azepan-1-yl)phenyl)diazenyl)-3,5-dimethylisoxazole

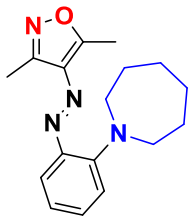

A mixture of (*E*)-4-((2-fluorophenyl)diazenyl)-3,5-dimethylisoxazole (44 mg, 0.2 mmol) in azepane (4 mL) was stirred overnight at 60 ^{o}C. The reaction mixture was washed with ethyl acetate and concentrated on rotary evaporator. The crude was purified by column chromatography on silica gel using distilled hexane to yield the product (51 mg, 0.17mmol, 86%) as orange solid.

Color: orange, **HRMS-ESI**: m/z $[M+H]^+$: 299.1864.

(*E*)-4-(2-((3,5-dimethylisoxazol-4-yl)diazenyl)-3-fluorophenyl)morpholine

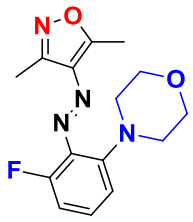

A mixture of (*E*)-4-((2,6-difluorophenyl)diazenyl)-3,5-dimethylisoxazole (50 mg, 0.2 mmol) and morpholine (86 µL, 1 mmol) in MeCN (2 mL) was stirred at 60 ^oC for 3 hrs. The reaction mixture was washed with ethyl acetate and concentrated on rotary evaporator. The crude was purified by column chromatography on silica gel using distilled hexane to yield the product (52 mg, 0.17mmol, 86%) as orange solid.

Color: orangr, ^1H NMR (400MHz, $CDCl_3$) δ2.52 (s, 3H), 2.74 (s, 3H), 3.07-3.09 (t, J= 8Hz, 4H), 3.79-3.81 (t, J= 8Hz, 4H), 6.82-6.87 (m, J= 20Hz, 2H), 7.23-7.26 (m, J= 12Hz, 1H).

IR (ATR, cm^{-1}): 727, 798, 998, 1106, 1235, 1364, 1406, 1595, 1731, 2819, 2967.

(*E*)-4-(2-((3,5-dimethylisoxazol-4-yl)diazenyl)phenyl)morpholine

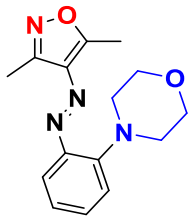

A mixture of (*E*)-4-((2-fluorophenyl)diazenyl)-3,5-dimethylisoxazole (200 mg, 0.9 mmol) in morpholine (16 mL) was stirred overnight at 67 ^oC. The reaction mixture was washed with ethyl acetate and concentrated on rotary evaporator. The crude was purified by column chromatography on silica gel using distilled hexane to yield the product (220 mg, 0.77 mmol, 85%) as orange solid.

Color: orange, ^{1}H NMR (400MHz, $CDCl_3$) δ 2.52 (s, 3H), 2.74 (s, 3H), 3.18-3.20 (t, J= 8Hz, 4H), 3.86-3.88 (t, J= 8hz, 4H), 7.01-7.08 (m, J= 28Hz, 2H), 7.35-7.39 (m, J= 16Hz, 1H), 7.53-7.55 (d, J= 12Hz, 1H); **HRMS-ESI**: m/z $[M+H]^+$: 287.1466.

IR (ATR, cm^{-1}): 764, 854, 921, 1044, 1119, 1221, 1278, 1409, 1482, 1592, 2834, 2854, 2921, 2967.

(*E*)-4-((2-fluoro-6-(piperazin-1-yl)phenyl)diazenyl)-3,5-dimethylisoxazole

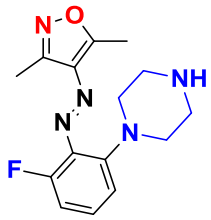

A mixture of (*E*)-4-((2,6-difluorophenyl)diazenyl)-3,5-dimethylisoxazole (50 mg, 0.2 mmol) and piperazine (86 mg, 1 mmol) in MeCN (2 mL) was stirred at room temperature for 8 hrs. The reaction mixture was washed with ethyl acetate and concentrated on rotary evaporator. The crude was purified by column chromatography on silica gel using distilled hexane to yield the product (46 mg, 0.15mmol, 76%) as orange solid.

(*E*)-3,5-dimethyl-4-((2-(piperazin-1-yl)phenyl)diazenyl)isoxazole

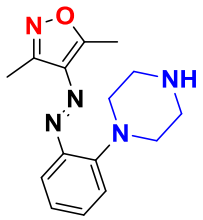

A mixture of (*E*)-4-((2-fluorophenyl)diazenyl)-3,5-dimethylisoxazole (200 mg, 0.46 mmol) and Piperazine (196 mg, 2.3 mmol) in MeCN (2 mL) was stirred at 70 ^{o}C for overnight. The reaction mixture was washed with ethyl acetate and concentrated on rotary evaporator. The crude was purified by column chromatography on silica gel using distilled hexane to yield the product (91 mg, 0.32 mmol, 70%) as orange solid.

(*E*)-4-((2-fluoro-6-(pyrrolidin-1-yl)phenyl)diazenyl)-1,3,5-trimethyl-1H-pyrazole

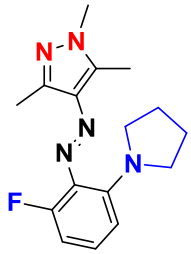

A mixture of (*E*)-4-((2,6-difluorophenyl)diazenyl)-1,3,5-trimethyl-1H-pyrazole (50 mg, 0.2 mmol) and pyrrolidine (82 µL, 1 mmol) in MeCN (2 mL) was stirred at RT for overnight. The reaction mixture was washed with ethyl acetate and concentrated on rotary evaporator. The crude was purified by column chromatography on silica gel using distilled hexane to yield the product (51 mg, 0.17, 85%) as orange solid.

Color: orange, **HRMS-ESI**: m/z $[M+H]^+$: 302.1757.

(*E*)-1,3,5-trimethyl-4-((2-(pyrrolidin-1-yl)phenyl)diazenyl)-1H-pyrazole

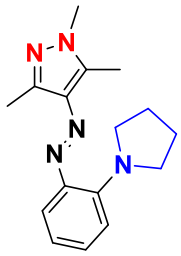

Method 1:

A mixture of (*E*)-4-((2-fluorophenyl)diazenyl)-1,3,5-trimethyl-1H-pyrazole (232 mg, 1 mmol), pyrrolidine (90.3 µL, 1.1 mmol) and K_2CO_3 (152 mg, 1.1 mmol) in MeCN (2 mL) was stirred for 1 hr at 80 ^oC. The reaction mixture was washed with ethyl acetate and concentrated on rotary evaporator. The crude was purified by column chromatography on silica gel using distilled hexane to yield the product (238 mg, 0.84mmol, 84%) as orange solid.

Method 2

A mixture of (*E*)-4-((2-fluorophenyl)diazenyl)-1,3,5-trimethyl-1H-pyrazole (50 mg, 0.21 mmol), pyrrolidine (2 mL) in MeCN (2 mL) was stirred overnight at 80 ^{o}C. The reaction mixture was washed with ethyl acetate and concentrated on rotary evaporator. The crude was purified by column chromatography on silica gel using distilled hexane to yield the product (49 mg, 0.17mmol, 83%) as orange solid.

Color: orange, ^{1}H NMR (400MHz, $CDCl_3$) δ1.92-1.95 (t, J= 12Hz, 4H), 2.45 (s, 3H), 2.54 (s, 3H), 3.52-3.55 (t, J= 12Hz, 4H), 3.77 (s, 3H) 6.69-6.72 (t, J= 12Hz, 1H), 6.79-6.81 (d, J= 8Hz, 1H), 7.19-7.22 (t, J= 12Hz, 1H), 7.48-7.50 (d, J= 8Hz, 1H); **HRMS-ESI**: m/z $[M-H]^{+}$: 282.1810.

IR (ATR, cm^{-1}): 741, 1036, 1168, 1552, 1596, 1731, 2852, 2924.

(*E*)-1-(3-fluoro-2-((1,3,5-trimethyl-1H-pyrazol-4-yl)diazenyl)phenyl)piperidine

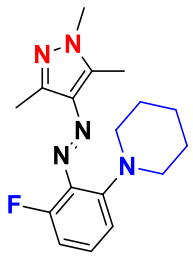

A mixture of (*E*)-4-((2,6-difluorophenyl)diazenyl)-1,3,5-trimethyl-1H-pyrazole (150 mg, 0.6 mmol) and piperidine (255 µL) in MeCN (2 mL) was stirred at RT for overnight. The reaction mixture was washed with ethyl acetate and concentrated on rotary evaporator. The crude was purified by column chromatography on silica gel using distilled hexane to yield the product (51 mg, 0.17, 85%) as orange solid.

(*E*)-1-(2-((1,3,5-trimethyl-1H-pyrazol-4-yl)diazenyl)phenyl)piperidine

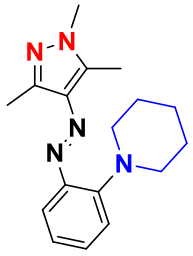

A mixture of (*E*)-4-((2-fluorophenyl)diazenyl)-1,3,5-trimethyl-1H-pyrazole (50 mg, 1 mmol) and piperidine (2 mL) in MeCN (2 mL) was stirred overnight at 80 ^{0}C. The reaction mixture was washed with ethyl acetate and concentrated on rotary evaporator. The crude was purified by column chromatography on silica gel using distilled hexane to yield the product (50mg, 0.17 mmol, 80%) as orange solid.

(*E*)-1-(3-fluoro-2-((1,3,5-trimethyl-1H-pyrazol-4-yl)diazenyl)phenyl)azepane

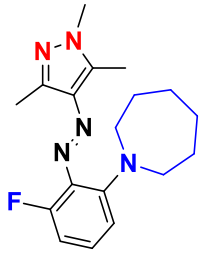

A mixture of (*E*)-4-((2,6-difluorophenyl)diazenyl)-1,3,5-trimethyl-1H-pyrazole (150 mg, 0.6 mmol) and pyrrolidine (298 µL) in MeCN (2 mL) was stirred at RT for overnight. The reaction mixture was washed with ethyl acetate and concentrated on rotary evaporator. The crude was purified by column chromatography on silica gel using distilled hexane to yield the product (51 mg, 0.17, 85%) as orange solid.

(*E*)-1-(2-((1,3,5-trimethyl-1H-pyrazol-4-yl)diazenyl)phenyl)azepane

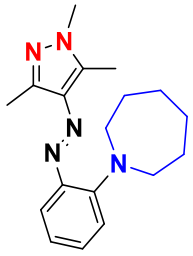

A mixture of (*E*)-4-((2-fluorophenyl)diazenyl)-1,3,5-trimethyl-1H-pyrazole (232 mg, 1 mmol) and azepane (2mL) in MeCN (2 mL) was stirred overnight at 80 ^{o}C. The reaction mixture was washed with ethyl acetate and concentrated on rotary evaporator. The crude was purified by column chromatography on silica gel using distilled hexane to yield the product (54 mg, 0.17mmol, 83%) as orange solid.

(*E*)-4-(3-fluoro-2-((1,3,5-trimethyl-1H-pyrazol-4-yl)diazenyl)phenyl)morpholine

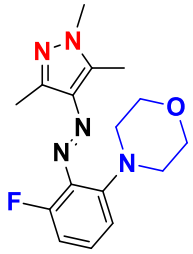

A mixture of (*E*)-4-((2,6-difluorophenyl)diazenyl)-1,3,5-trimethyl-1H-pyrazole (50 150 mg, 0.6 mmol) and pyrrolidine (259 µL) in MeCN (2 mL) was stirred at RT for overnight. The reaction mixture was washed with ethyl acetate and concentrated on rotary evaporator. The crude was purified by column chromatography on silica gel using distilled hexane to yield the product (51 mg, 0.17, 85%) as orange solid.

Color: orange, ^{1}H NMR (400MHz, $CDCl_3$) δ 2.49 (s, 3H), 2.56 (s, 3H), 3.08-3.10 (t, J= 8Hz, 4H), 3.79-3.80 (m, J= 4Hz, 7H), 6.80-6.85 (m, J= 20Hz, 2H), 7.15-7.17 (d of d, J= 8Hz, 1H).

(*E*)-4-(2-((1,3,5-trimethyl-1H-pyrazol-4-yl)diazenyl)phenyl)morpholine

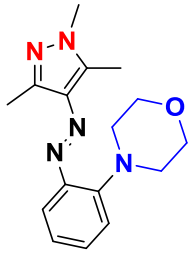

A mixture of (*E*)-4-((2-fluorophenyl)diazenyl)-1,3,5-trimethyl-1H-pyrazole (232 mg, 1 mmol) and morpholine (2 mL) in MeCN (2 mL) was stirred overnight at 80 ^{o}C. The reaction mixture was washed with ethyl acetate and concentrated on rotary evaporator. The crude was purified by column chromatography on silica gel using distilled hexane to yield the product (53mg, 0.18mmol, 84%) as orange solid.

References

1. Bafana, A.; Devi, S. S.; Chakrabarti, T. *Environ. Rev.* **2011**, *19* (NA), 350–371.

2. Welham, R. D. *J. Soc. Dyers Colour.* **2008**, *79* (3), 98–105.

3. Piao, W.; Tsuda, S.; Tanaka, Y.; Maeda, S.; Liu, F.; Takahashi, S.; Kushida, Y.; Komatsu, T.; Ueno, T.; Terai, T.; Nakazawa, T.; Uchiyama, M.; Morokuma, K.; Nagano, T.; Hanaoka, K. *Angew. Chem. Int. Ed.* **2013**, *52* (49), 13028–13032.

4. Ali, Y.; Hamid, S. A.; Rashid, U. *Mini. Rev. Med. Chem.* **2018**, *18* (18), 1548–1558.

5. Dembitsky, V. M.; Gloriozova, T. A.; Poroikov, V. V. *Nat. Prod. Bioprospect.* **2017**, *7*(1), 151–169.

6. Shin, N.; Hanaoka, K.; Piao, W.; Miyakawa, T.; Fujisawa, T.; Takeuchi, S.; Takahashi, S.; Komatsu, T.; Ueno, T.; Terai, T.; Tahara, T.; Tanokura, M.; Nagano, T.; Urano, Y. *ACS Chem. Biol.* **2017**, *12* (2), 558–563.

7. Yilmaz, M. D.; Oktem, H. A. *Anal. Chem.***2018**, *90* (6), 4221–4225.

8. Hickman, K. C. D.; Linstead, R. P. *J. Chem. Soc., Trans.***1922**, *121*, 2502–2506.

9. Hartley, G. S. *Nat.* **1937**, *140* (3537), 281–281.

10. Merino, E.; Ribagorda, M. *Beilstein J. Org. Chem.* **2012**, *8*, 1071–1090.

11. Bandara, H. M. D.; Burdette, S. C. *Chem. Soc. Rev.***2012**, *41* (5), 1809–1825.

12. Stuart, C. M.; Frontiera, R. R.; Mathies, R. A. *J. Phys. Chem. A* **2007**, *111* (48), 12072–12080.

13. Chang, C.-W.; Lu, Y.-C.; Wang, T.-T.; Diau, E. W.-G. *J. Am. Chem. Soc.* **2004**, *126* (32), 10109–10118.

14. Tan, E. M. M.; Amirjalayer, S.; Smolarek, S.; Vdovin, A.; Zerbetto, F.; Buma, W. J. *Nat. Commun.* **2015**, *6* (1).

15. Crecca, C. R.; Roitberg, A. E. *J. Phys. Chem. A* **2006**, *110* (26), 8188–8203.

16. Bello, K. A.; Griffiths, J. *J. Chem. Soc., Chem. Commun.* **1986**, No. 22, 1639

17. Salvador, M. A.; Almeida, P.; Reis, L.; Santos, P. *Dyes Pigm.* **2009**, *82* (2), 118–123.

18. Whitten, D. G.; Wildes, P. D.; Pacifici, J. G.; Irick, G. *J. Am. Chem. Soc.* **1971**, *93* (8), 2004–2008.

19. Shinkai, S.; Nakaji, T.; Ogawa, T.; Shigematsu, K.; Manabe, O. *J. Am. Chem. Soc.* **1981**, *103* (1), 111–115.

20. Haberfield, P.; Block, P. M.; Lux, M. S. *J. Am. Chem. Soc.* **1975**, *97* (20), 5804–5806.

21. Nishimura, N.; Sueyoshi, T.; Yamanaka, H.; Imai, E.; Yamamoto, S.; Hasegawa, S. *Bull. Chem. Soc. Jpn.* **1976**, *49* (5), 1381–1387.

22. Siewertsen, R.; Neumann, H.; Buchheim-Stehn, B.; Herges, R.; Näther Christian; Renth, F.; Temps, F. *J. Am. Chem. Soc.* **2009**, *131* (43), 15594–15595.

23. Li, Y.; Patrick, B. O.; Dolphin, D. *J. Org. Chem.* **2009**, *74* (15), 5237–5243.

24. Yang, Y.; Hughes, R. P.; Aprahamian, I. *J. Am. Chem. Soc.* **2012**, *134* (37), 15221–15224.

25. Yang, Y.; Hughes, R. P.; Aprahamian, I. *J. Am. Chem. Soc.* **2014**, *136* (38), 13190–13193.

26. Bushuyev, O. S.; Tomberg, A.; Friščić, T.; Barrett, C. J. *J. Am. Chem. Soc.* **2013**, *135* (34), 12556–12559.

27. Bushuyev, O. S.; Corkery, T. C.; Barrett, C. J.; Friščić, T *Chem. Sci.***2014**, *5* (8), 3158–3164.

28. Beharry, A. A.; Sadovski, O.; Woolley, G. A. *J. Am. Chem. Soc.* **2011**, *133*(49), 19684–19687.

29. Quick, M.; Berndt, F.; Dobryakov, A. L.; Ioffe, I. N.; Granovsky, A. A.; Knie, C.; Mahrwald, R.; Lenoir, D.; Ernsting, N. P.; Kovalenko, S. A. *J. Phys. Chem. B* **2014**, *118* (5), 1389–1402.

30. Ebadi, H. *J. Phys. Chem. A* **2014**, *118* (36), 7832–7837.

31. Corchado, J. C.; Sánchez, M. L.; Galván, I. F.; Martín, M. E.; Muñoz-Losa, A.; Barata-Morgado, R.; Aguilar, M. A. *J. Phys. Chem. B* **2014**, *118* (43), 12518–12530.

32. Ikegami, T.; Kurita, N.; Sekino, H.; Ishikawa, Y. *J. Phys. Chem. A* **2003**, *107* (22), 4555–4562.

33. Calbo, J.; Weston, C. E.; White, A. J. P.; Rzepa, H. S.; Contreras-García, J.; Fuchter, M. J. *J. Am. Chem. Soc.* **2017**, *139* (3), 1261–1274.

34. Wendler, T.; Schütt, C.; Näther, C.; Herges, R. *J. Org. Chem.* **2012**, *77* (7), 3284–3287.

35. Ahmed, Z.; Siiskonen, A.; Virkki, M.; Priimagi, A. *Chem. Commun.***2017**, *53* (93), 12520–12523.

36. Hampson, G. C.; Robertson, J. M. *J. Chem. Soc. (Resumed)* **1941**, 409.

37. Weston, C. E.; Richardson, R. D.; Haycock, P. R.; White, A. J. P.; Fuchter, M. J. *J. Am. Chem. Soc.* **2014**, *136* (34), 11878–11881.

38. Croissant, J.; Maynadier, M.; Gallud, A.; Peindy Ndongo, H.; Nyalosaso, J. L.; Derrien, G.; Charnay, C.; Durand, J.-O.; Raehm, L.; Serein-Spirau, F.; Cheminet, N.; Jarrosson, T.; Mongin, O.; Blanchard-Desce, M.; Gary-Bobo, M.; Garcia, M.; Lu, J.; Tamanoi, F.; Tarn, D.; Guardado-Alvarez, T. M.; Zink, J. I. *Angew. Chem. Int. Ed.* **2013**, *52* (51), 13813–13817.

39. Venkataramani, S.; Jana, U.; Dommaschk, M.; Sonnichsen, F. D.; Tuczek, F.; Herges, R. *Science* **2011**, *331* (6016), 445–448.

40. Wu, W.; Yao, L.; Yang, T.; Yin, R.; Li, F.; Yu, Y. *J. Am. Chem. Soc.* **2011**, *133*(40), 15810–15813.

41. Jiang, Z.; Xu, M.; Li, F.; Yu, Y. *J. Am. Chem. Soc.* **2013**, *135* (44), 16446–16453.

42. Siewertsen, R.; Neumann, H.; Buchheim-Stehn, B.; Herges, R.; Näther Christian; Renth, F.; Temps, F. *J. Am. Chem. Soc.* **2009**, *131* (43), 15594–15595.

43. Samanta, S.; Beharry, A. A.; Sadovski, O.; Mccormick, T. M.; Babalhavaeji, A.; Tropepe, V.; Woolley, G. A. *J. Am. Chem. Soc.* **2013**, *135* (26), 9777–9784.

44. Samanta, S.; Mccormick, T. M.; Schmidt, S. K.; Seferos, D. S.; Woolley, G. A. *Chem. Commun.***2013**, *49* (87), 10314.

45. Bléger, D.; Schwarz, J.; Brouwer, A. M.; Hecht, S. *J. Am. Chem. Soc.* **2012**, *134* (51), 20597–20600.

46. Hansch, C.; Leo, A.; Taft, R. W. *Chem. Rev.***1991**, *91* (2), 165–195.

47. Sadovski, O.; Beharry, A. A.; Zhang, F.; Woolley, G. A. *Angew. Chem. Int. Ed.* **2009**, *48* (8), 1484–1486.

48. Xu, Y.; Gao, C.; Andréasson, J.; Grøtli, M. *Org. Lett.***2018**, *20* (16), 4875–4879.

49. Diener, H.; Zollinger, H. *Can. J. Chem.* **1986**, *64* (6), 1102–1107.

50. Ahmed, Z.; Siiskonen, A.; Virkki, M.; Priimagi, A. *Chem. Commun.***2017**, *53* (93), 12520–12523.

51. Badger, G. M.; Cook, J. W.; Vidal, W. P.; Hodgson, H. H.; Ward, E. R. *J. Chem. Soc. (Resumed)* **1947**, 1109.

52. Manka, J. T.; Mckenzie, V. C.; Kaszynski, P. *J. Org. Chem.* **2004**, *69* (6), 1967–1971.

53. Bandara, H. M. D.; Burdette, S. C. *Chem. Soc. Rev.***2012**, *41* (5), 1809–1825.

Appendix 5A:

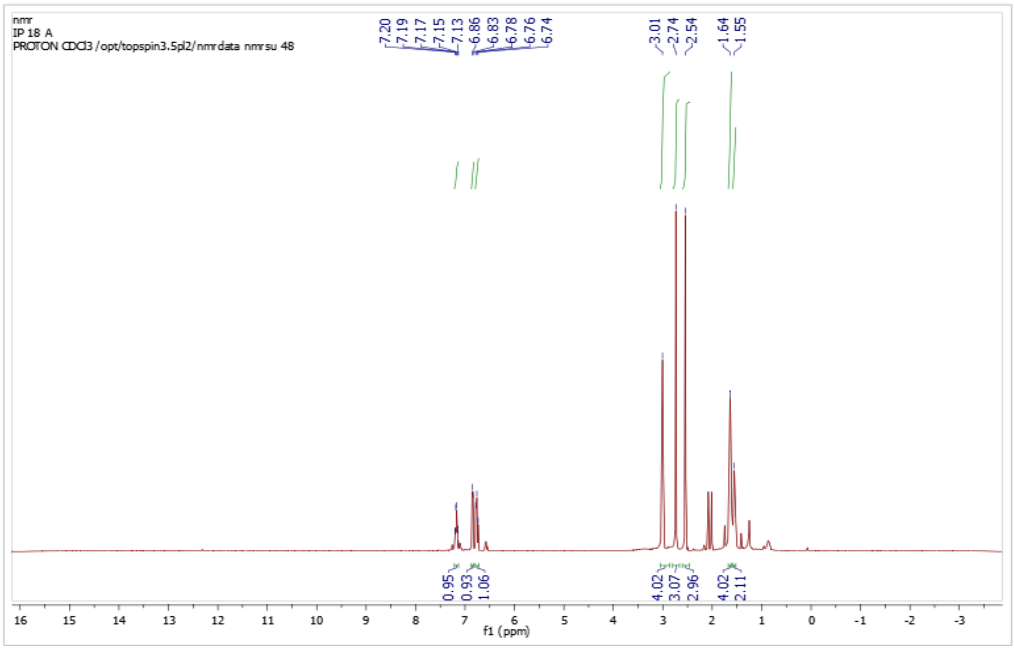

Fig. 5A.1 ^{1}H NMR of (*E*)-4-((2-fluoro-6-(piperidin-1-yl)phenyl)diazenyl)-3,5-dimethylisoxazole

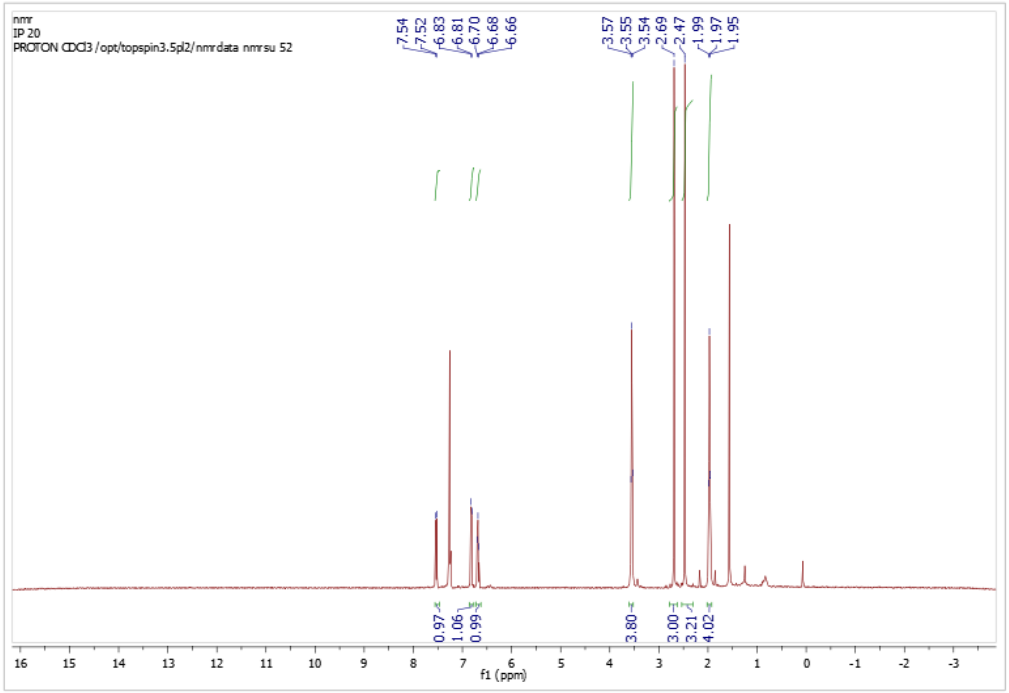

Fig. 5A.2 ^{1}H NMR of (*E*)-3,5-dimethyl-4-((2-(pyrrolidin-1-yl)phenyl)diazenyl)isoxazole

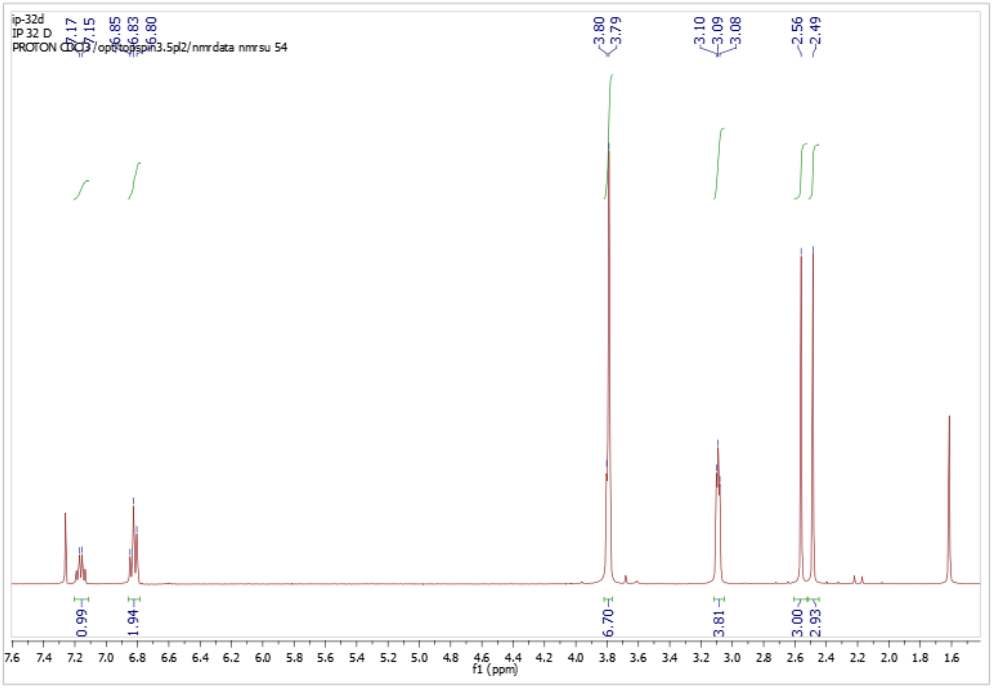

Fig. 5A.3 ^{1}H NMR of (*E*)-4-(3-fluoro-2-((1,3,5-trimethyl-1H-pyrazol-4-yl)diazenyl)phenyl)morpholine

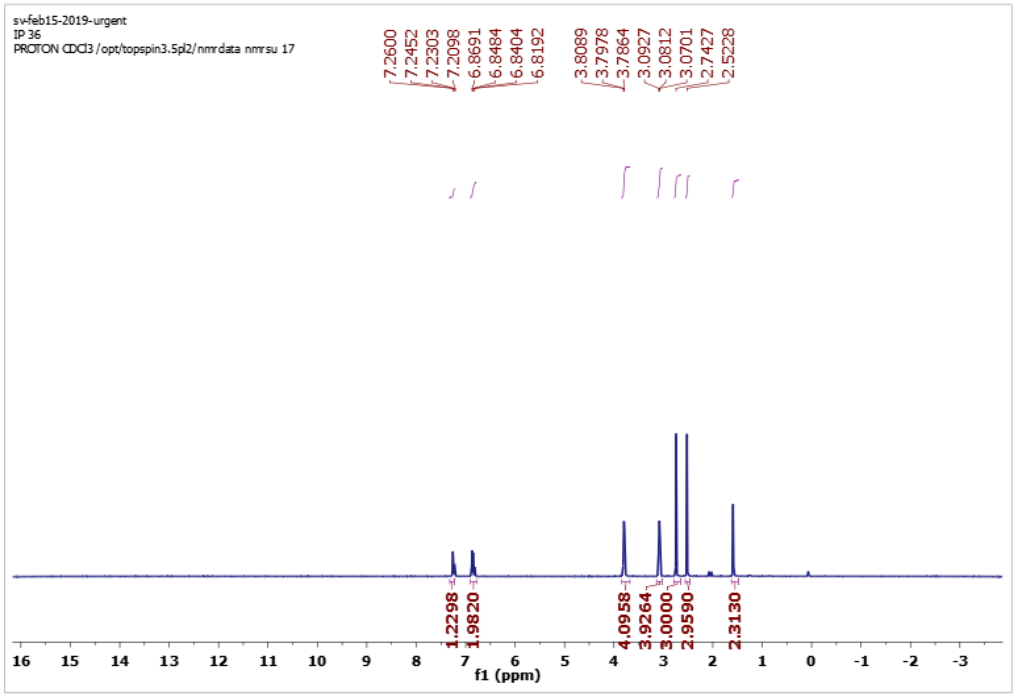

Fig. 5A.4 ^{1}H NMR of (*E*)-4-(2-((3,5-dimethylisoxazol-4-yl)diazenyl)-3-fluorophenyl)morpholine

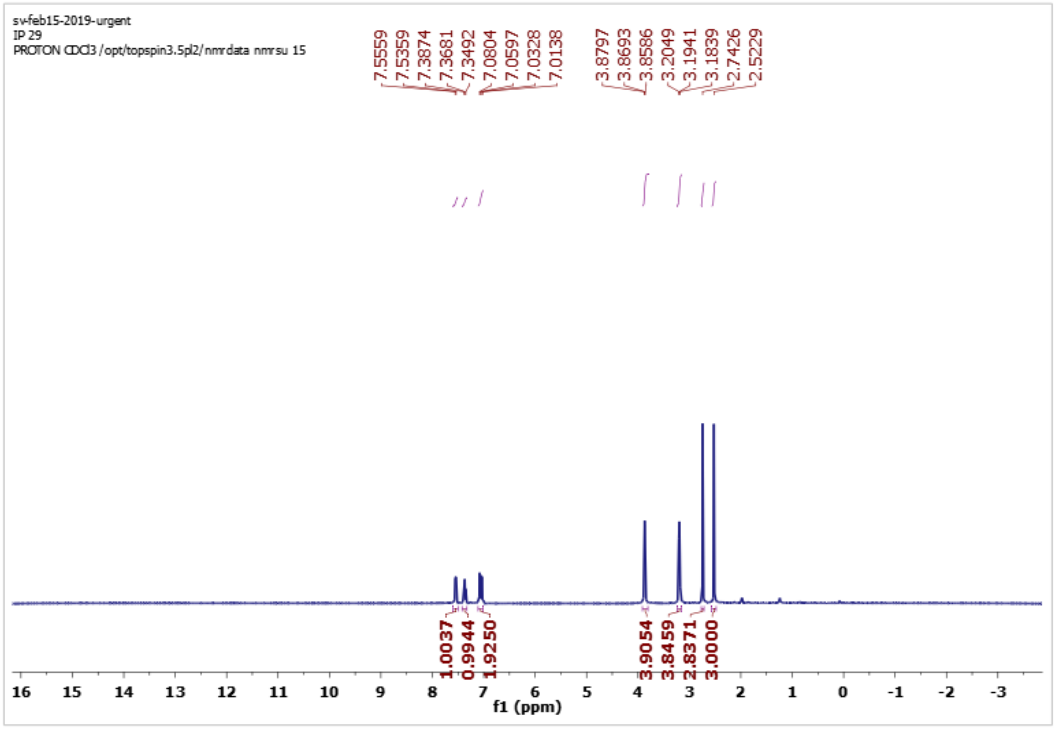

Fig. 5A.5 ^{1}H NMR of (*E*)-4-(2-((3,5-dimethylisoxazol-4-yl)diazenyl)phenyl)morpholine

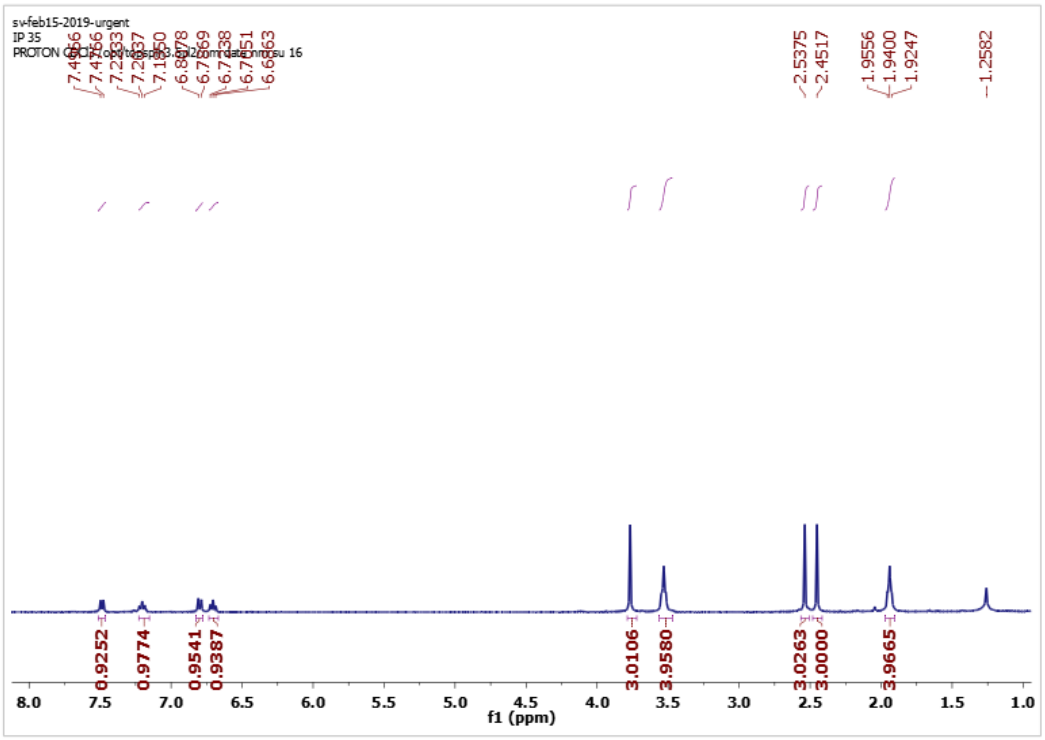

Fig. 5A.6 ^{1}H NMR of (*E*)-1,3,5-trimethyl-4-((2-(pyrrolidin-1-yl)phenyl)diazenyl)-1H-pyrazole

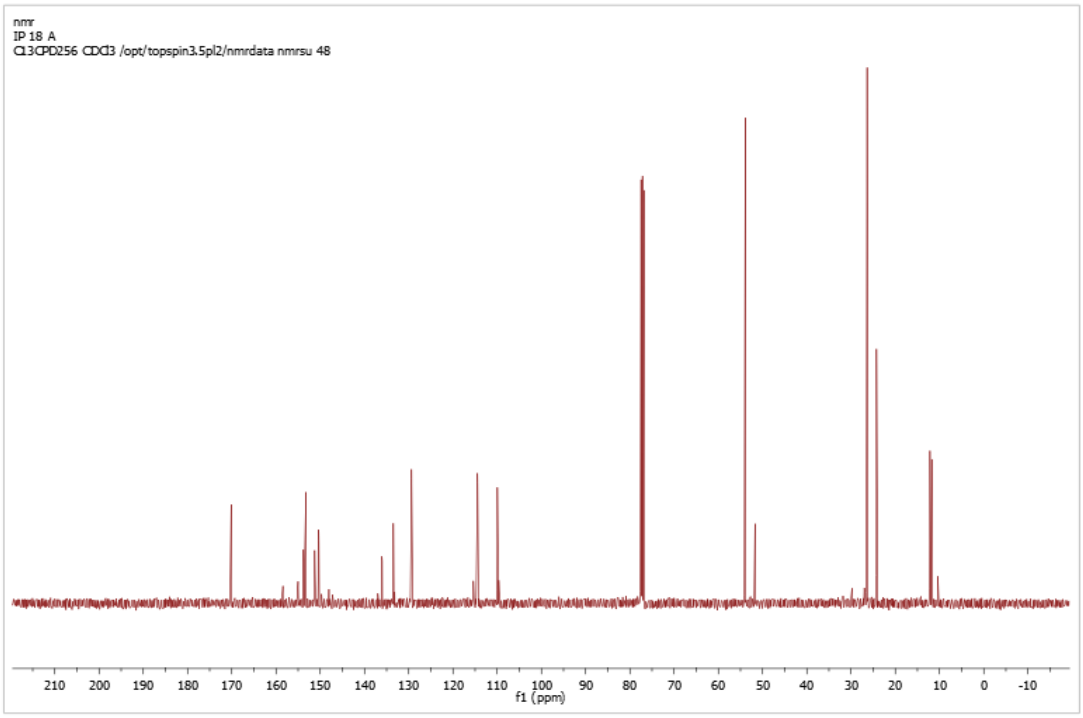

Fig. 5A.7 ^{13}C NMR of (*E*)-4-((2-fluoro-6-(piperidin-1-yl)phenyl)diazenyl)-3,5-dimethylisoxazole

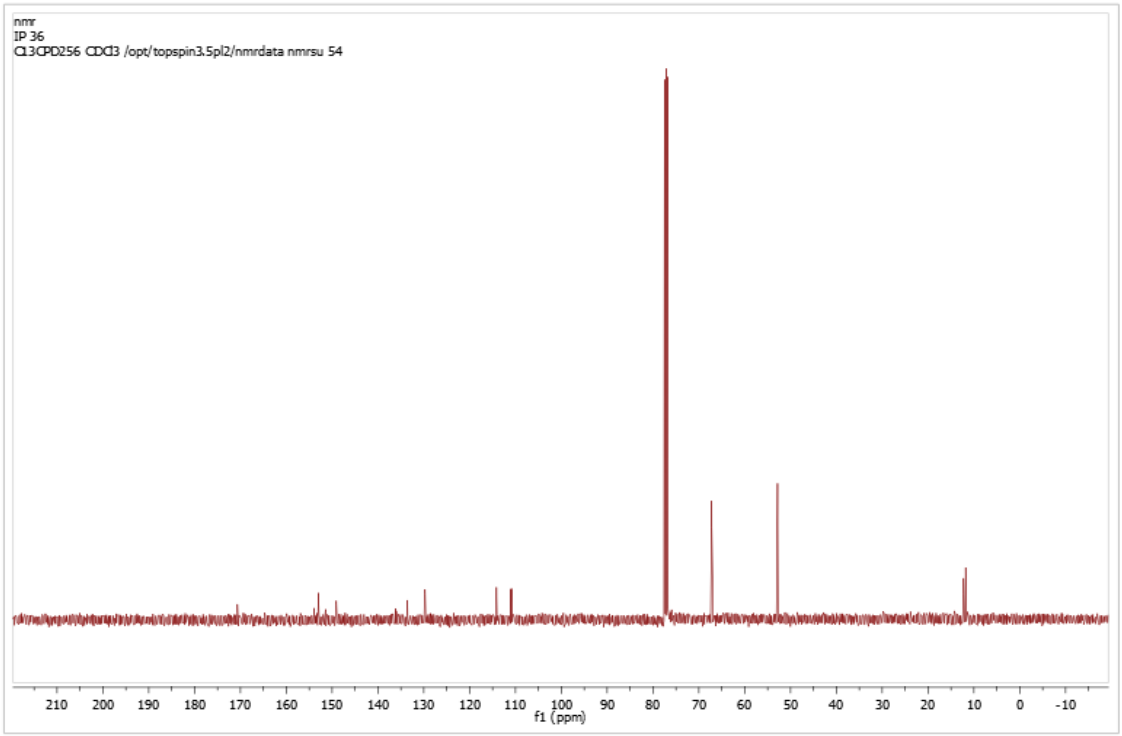

Fig. 5A.8 ^{13}C NMR of (*E*)-4-(2-((3,5-dimethylisoxazol-4-yl)diazenyl)-3-fluorophenyl)morpholine

Appendix 5B:

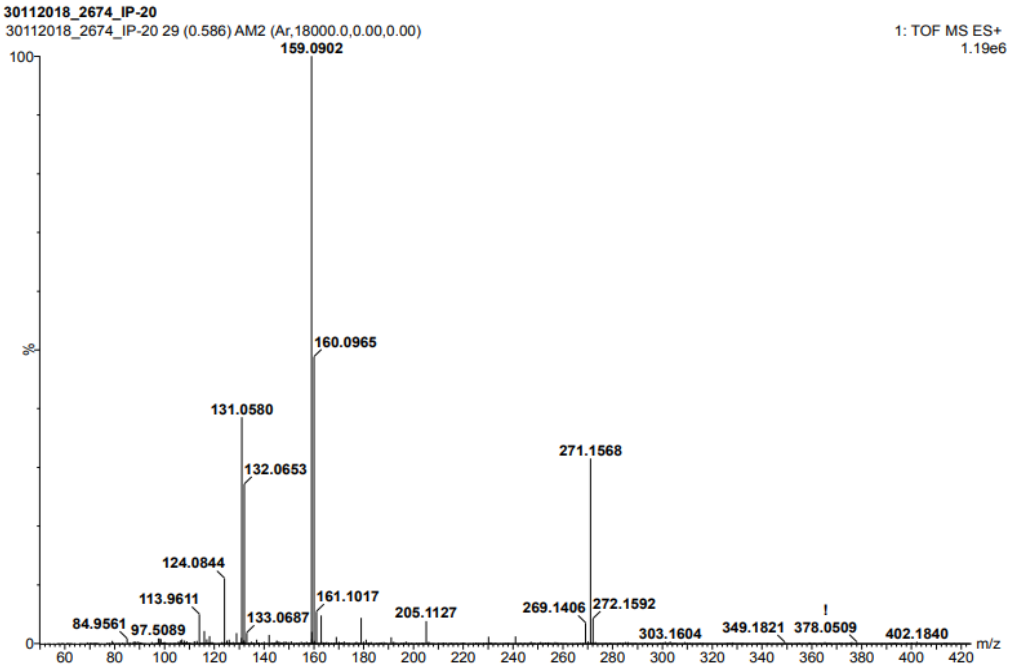

Fig. 5B.1 HRMS spectrum of (*E*)-3,5-dimethyl-4-((2-(pyrrolidin-1-yl)phenyl)diazenyl)isoxazole

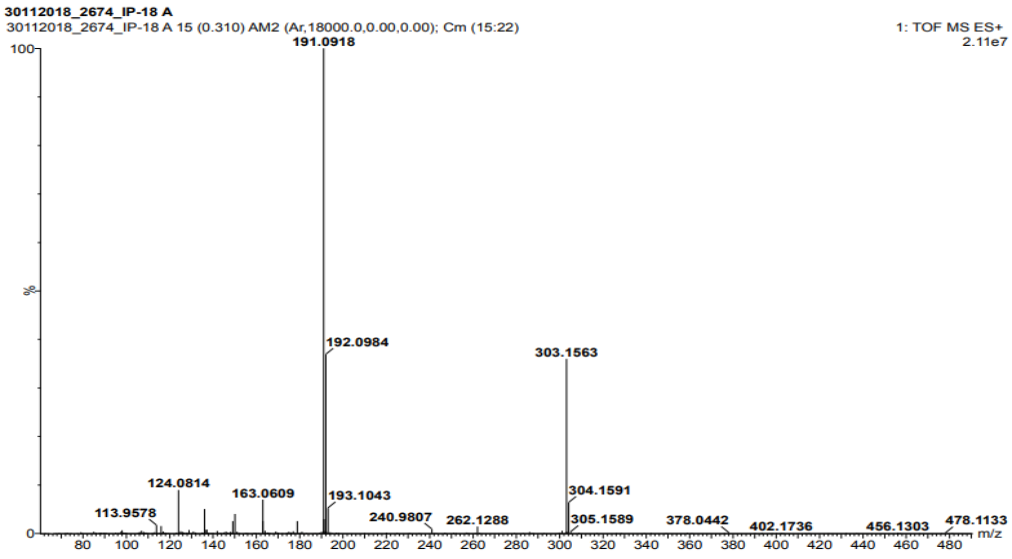

Fig. 5B.2 HRMS spectrum of (*E*)-4-((2-fluoro-6-(piperidin-1-yl)phenyl)diazenyl)-3,5-dimethylisoxazole

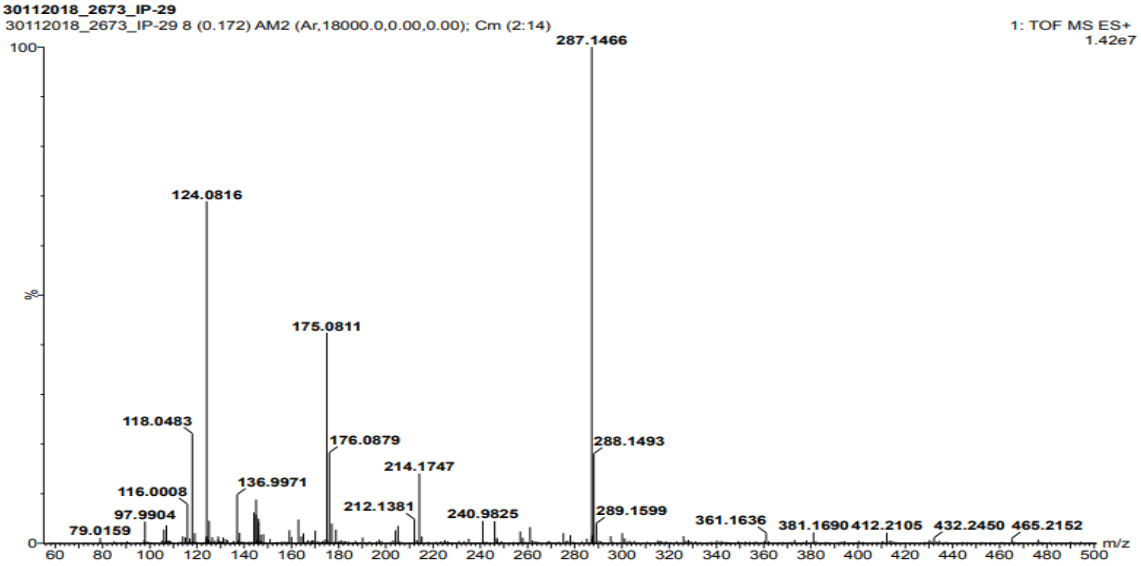

Fig. 5B.3 HRMS spectrum of (*E*)-4-(2-((3,5-dimethylisoxazol-4-yl)diazenyl)phenyl)morpholine

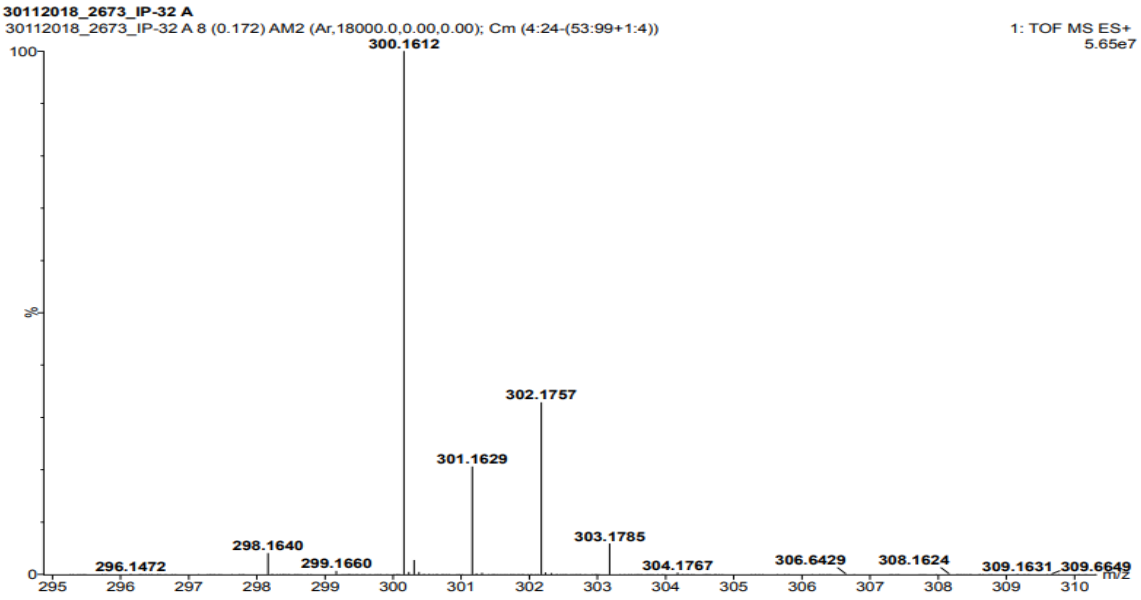

Fig. 5B.4 HRMS spectrum of (*E*)-4-((2-fluoro-6-(pyrrolidin-1-yl)phenyl)diazenyl)-1,3,5-trimethyl-1H-pyrazole

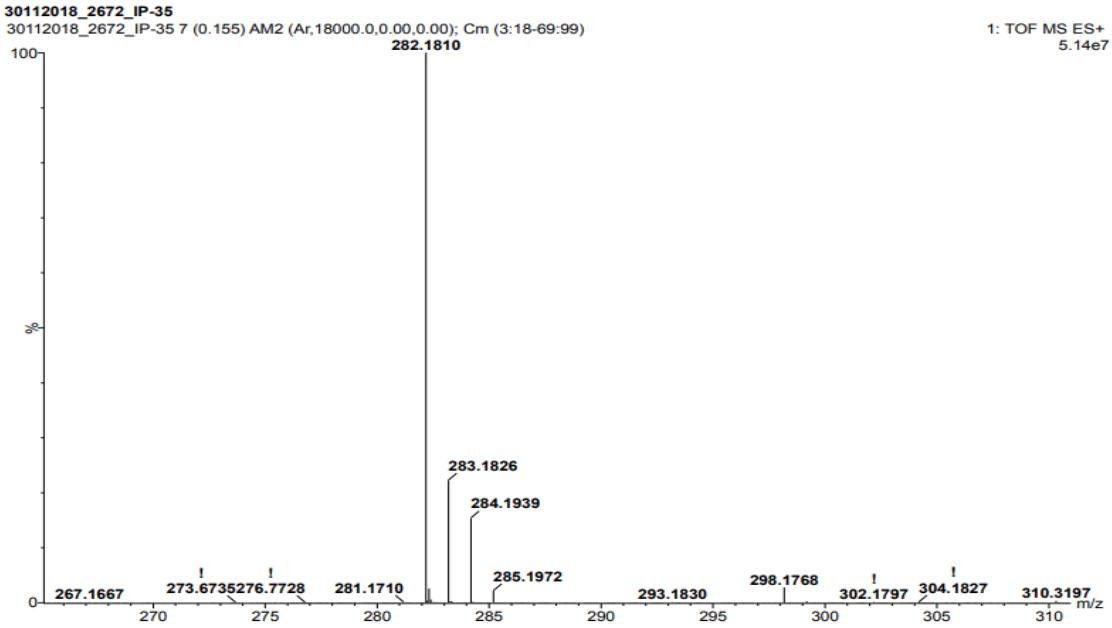

Fig. 5B.5 HRMS spectrum of (*E*)-1,3,5-trimethyl-4-((2-(pyrrolidin-1-yl)phenyl)diazenyl)-1H-pyrazole

Appendix 5C:

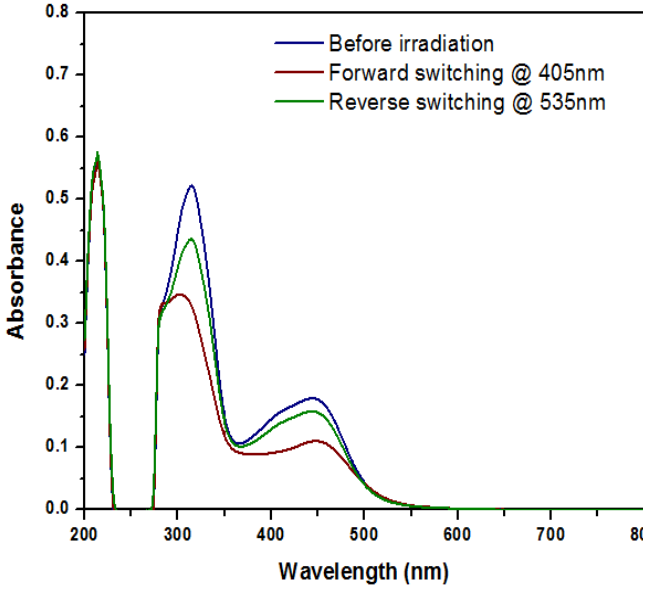

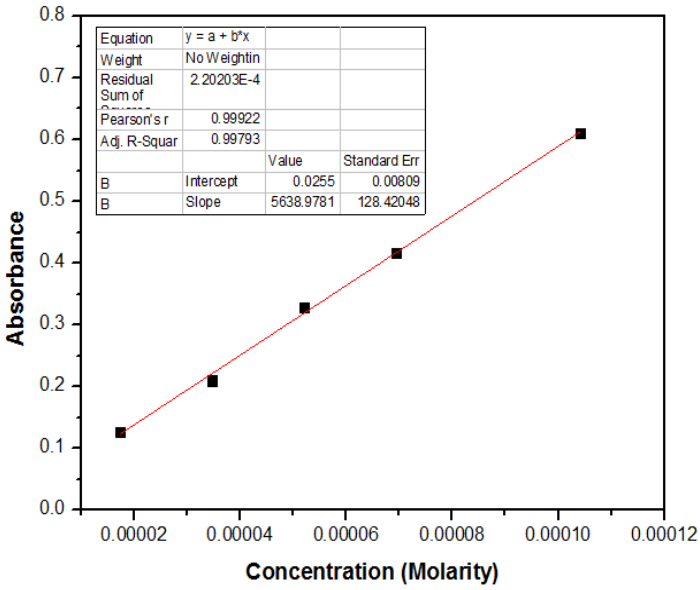

(a) (b)

Fig. 5C.1 UV-Vis photoswitching studies of **1f** (a) in CH_3CN solvent; Estimation of molar extinction coefficient (in CH_3CN) for the (b) π-π* absorption.

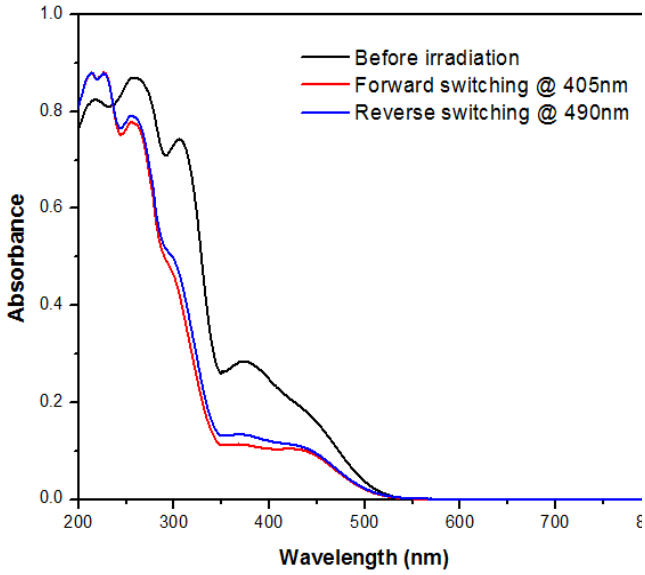

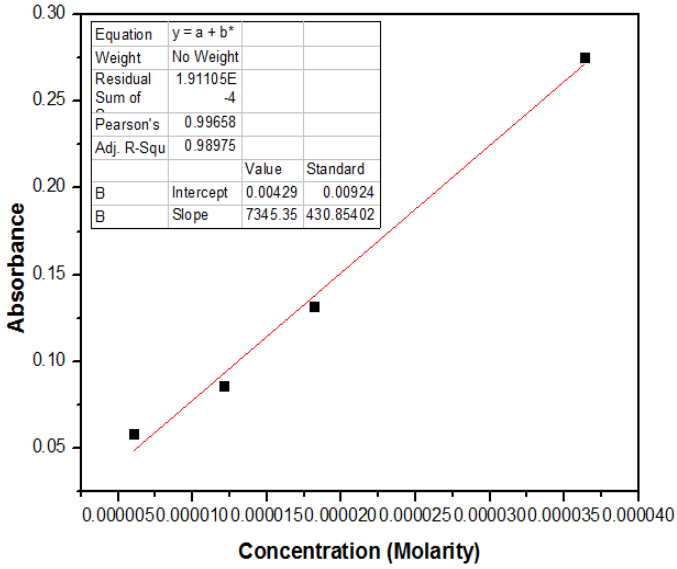

(a) (b)

Fig. 5C.2 UV-Vis photoswitching studies of **1g** (a) in CH_3CN solvent; Estimation of molar extinction coefficient (in CH_3CN) for the (b) π–π* absorption.

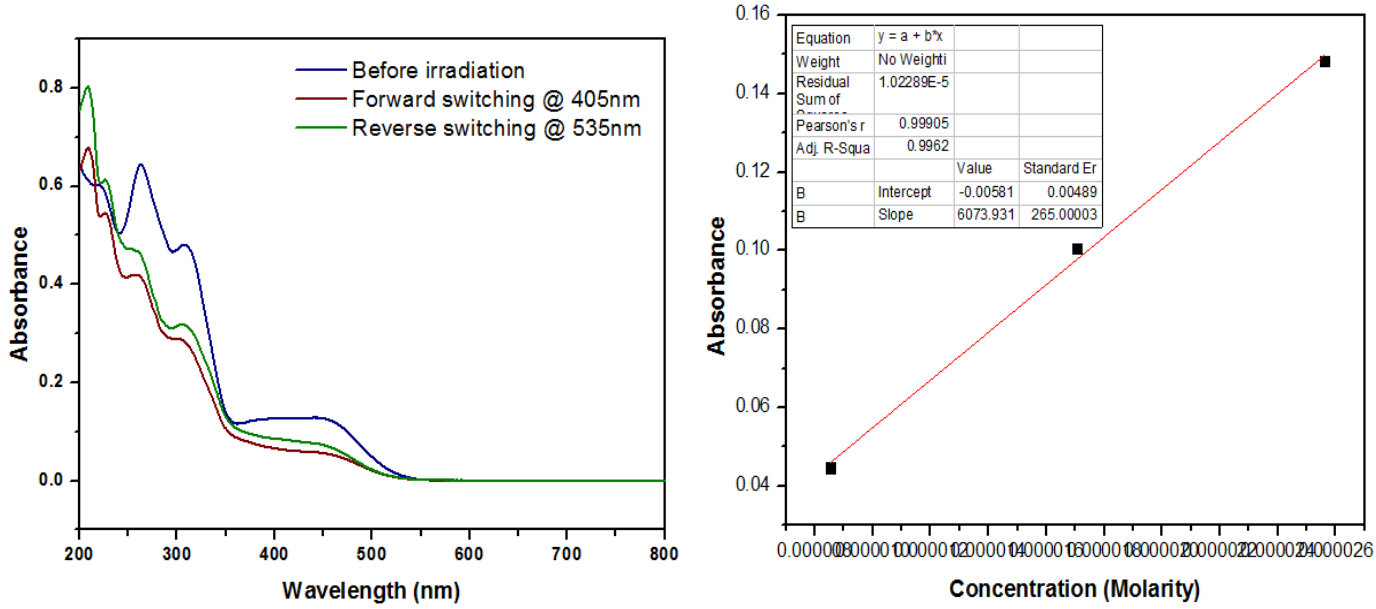

(a) (b)

Fig. 5C.3 UV-Vis photoswitching studies of **1h** (a) in CH_3CN solvent; Estimation of molar extinction coefficient (in CH_3CN) for the (b) $\pi-\pi^*$ absorption.

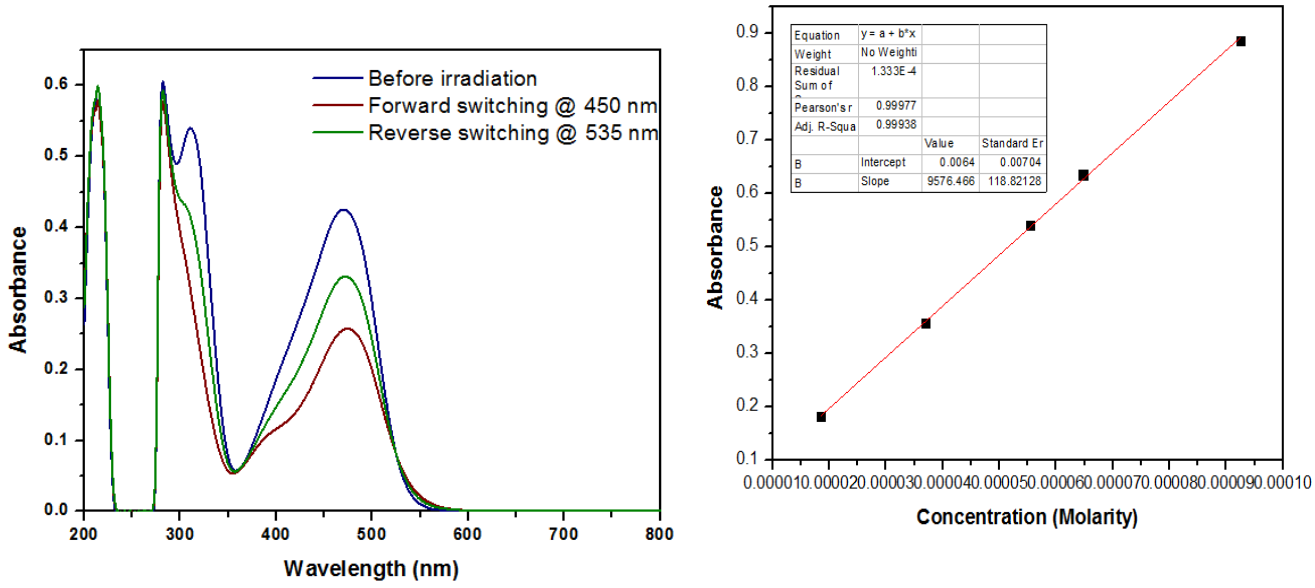

(a) (b)

Fig. 5C.4 UV-Vis photoswitching studies of **1a** (a) in CH_3CN solvent; Estimation of molar extinction coefficient (in CH_3CN) for the (b) π-π^* absorption.

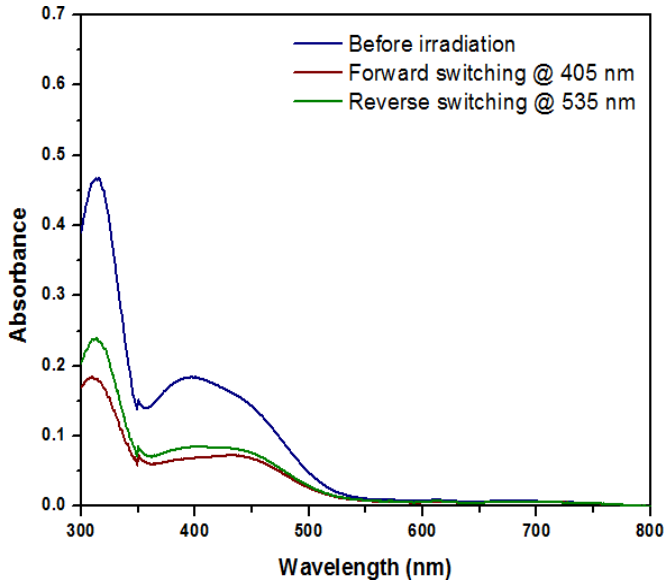

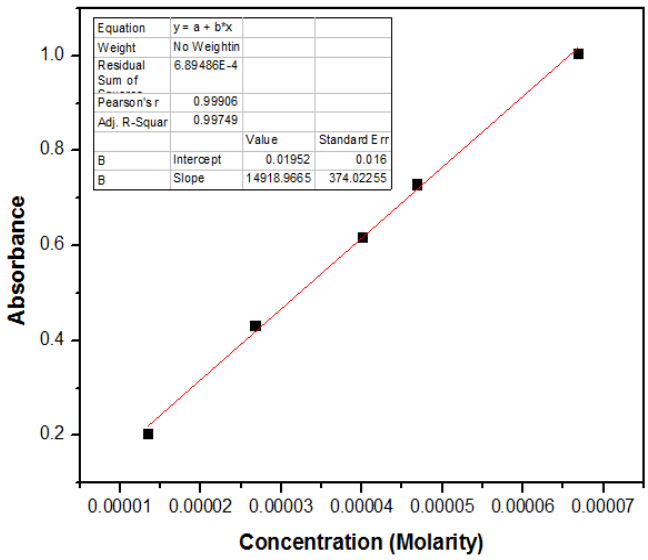

(a) (b)

Fig. 5C.5 UV-Vis photoswitching studies of **1b** (a) in CH_3CN solvent; Estimation of molar extinction coefficient (in CH_3CN) for the (b) π-π* absorption.

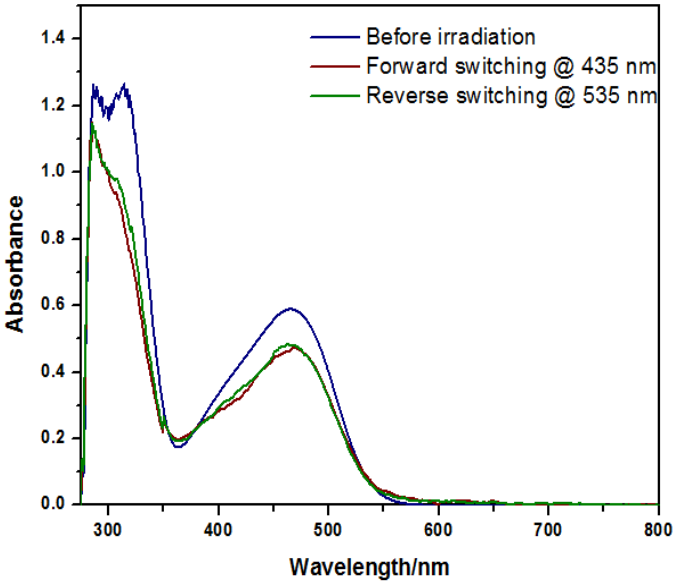

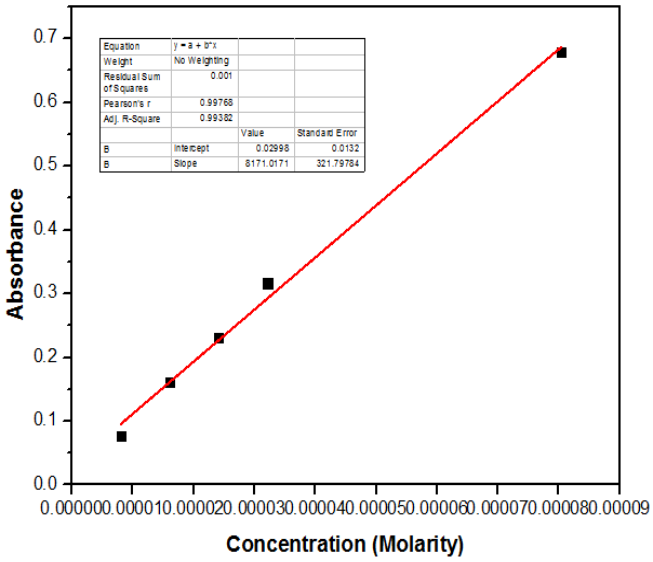

(a) (b)

Fig. 5C.6 UV-Vis photoswitching studies of **1c** (a) in CH_3CN solvent; Estimation of molar extinction coefficient (in CH_3CN) for the (b) π-π* absorption.

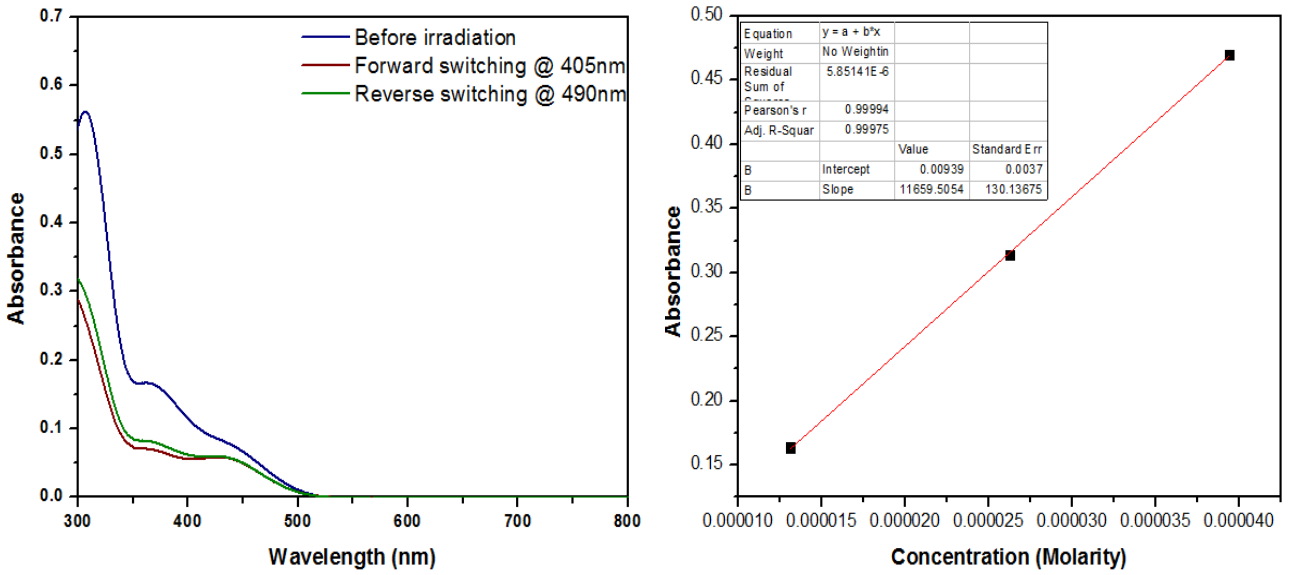

(a) (b)

Fig. 5C.7 UV-Vis photoswitching studies of **1i** (a) in CH_3CN solvent; Estimation of molar extinction coefficient (in CH_3CN) for the (b) π-π* absorption.

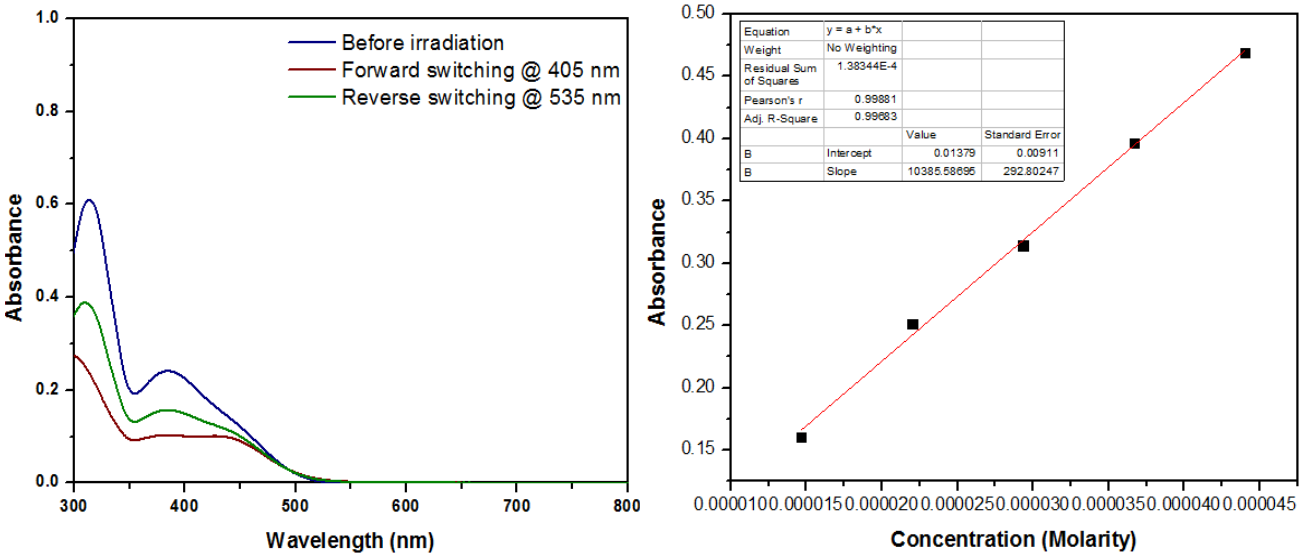

(a) (b)

Fig. 5C.8 UV-Vis photoswitching studies of **1d** (a) in CH_3CN solvent; Estimation of molar extinction coefficient (in CH_3CN) for the (b) π-π* absorption.

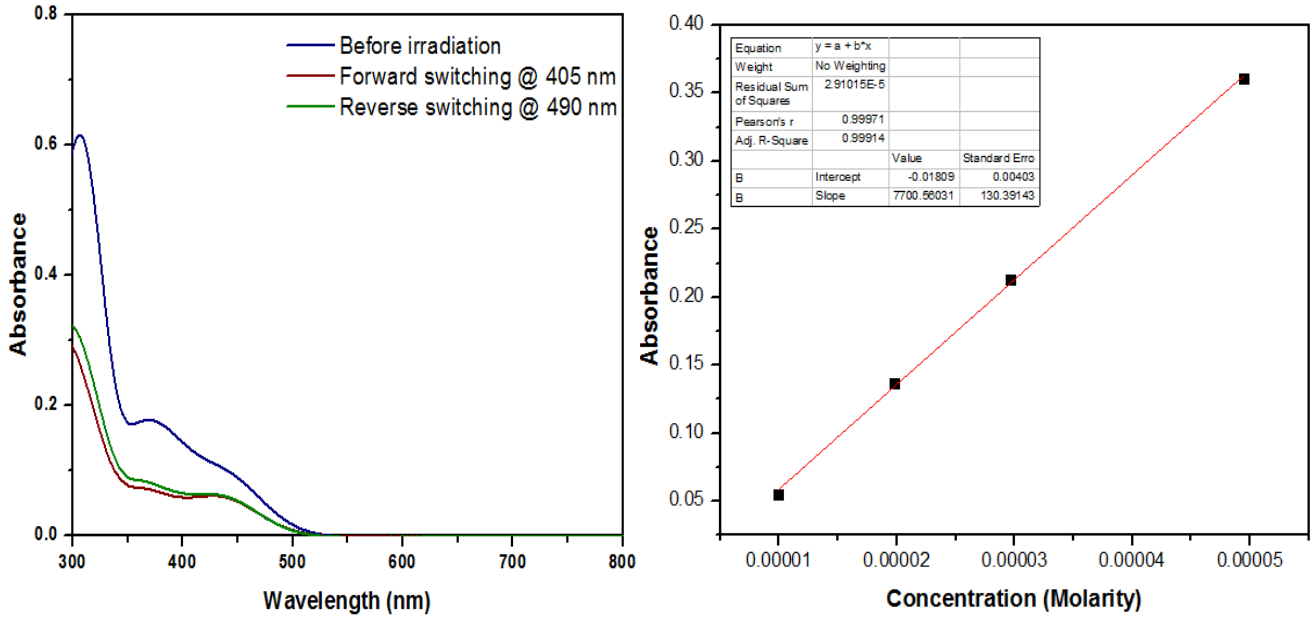

(a) (b)

Fig. 5C.9 UV-Vis photoswitching studies of **1j** (a) in CH_3CN solvent; Estimation of molar extinction coefficient (in CH_3CN) for the (b) π-π* absorption.

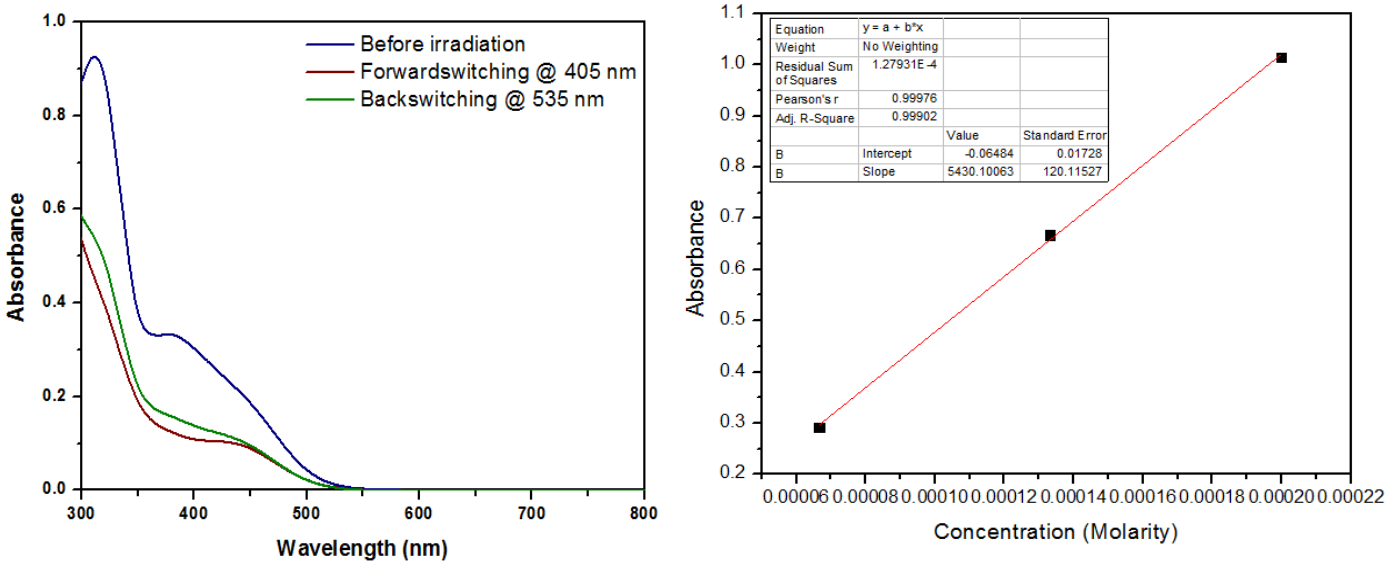

(a) (b)

Fig. 5C.10 UV-Vis photoswitching studies of **1e** (a) in CH_3CN solvent; Estimation of molar extinction coefficient (in CH_3CN) for the (b) π-π* absorption.

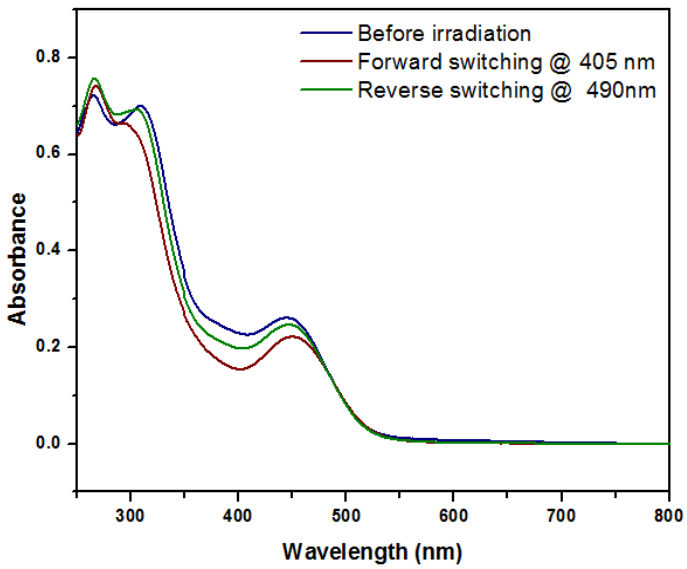

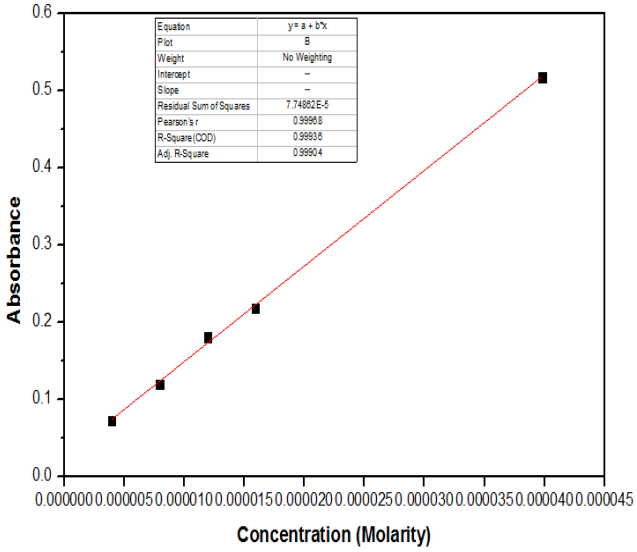

(a) (b)

Fig. 5C.11 UV-Vis photoswitching studies of **2f** (a) in CH_3CN solvent; Estimation of molar extinction coefficient (in CH_3CN) for the (b) π-π* absorption.

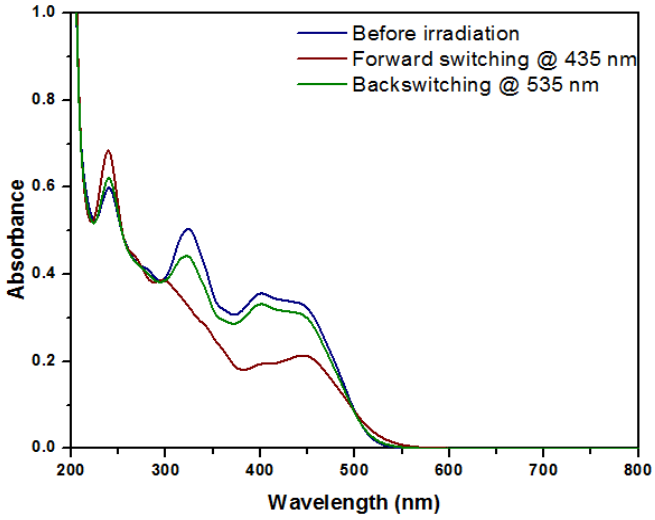

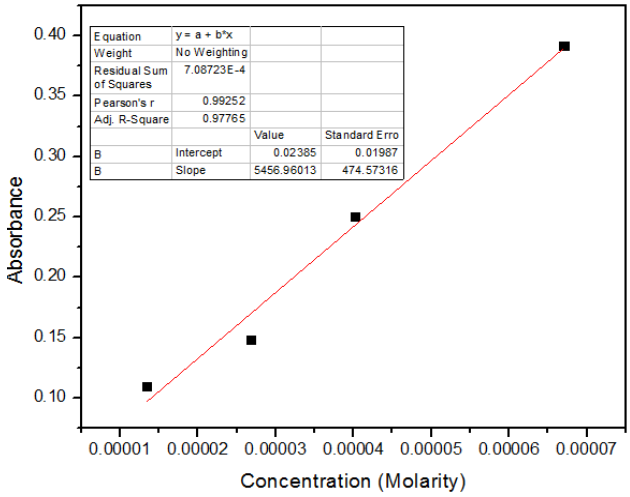

(a) (b)

Fig. 5C.12 UV-Vis photoswitching studies of **2a** (a) in CH_3CN solvent; Estimation of molar extinction coefficient (in CH_3CN) for the (b) π-π* absorption.

Appendix 5D

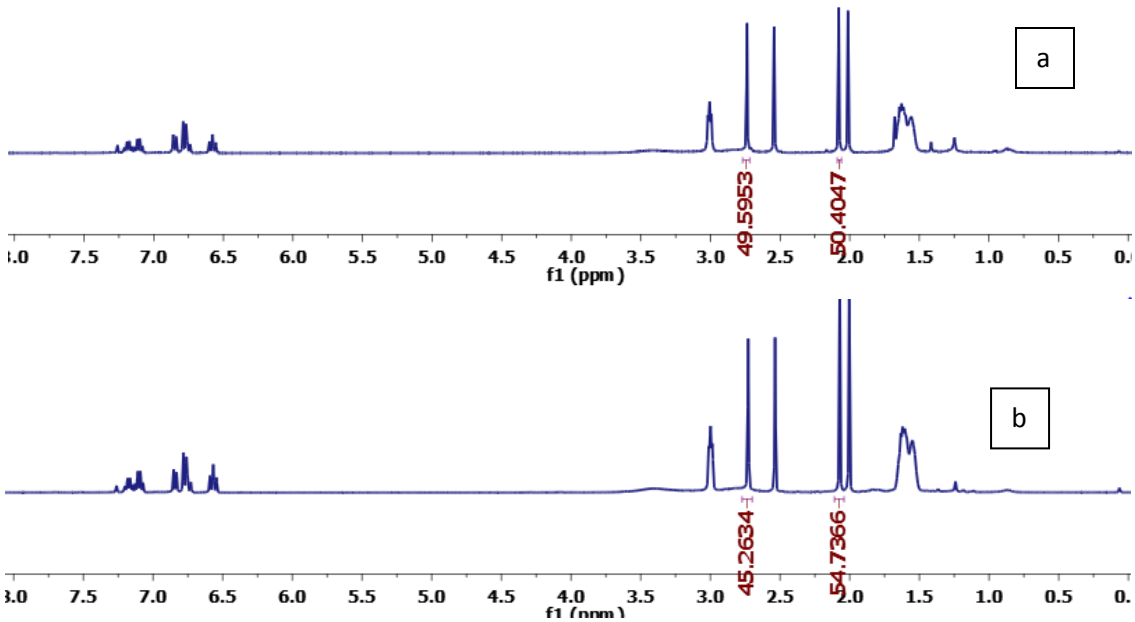

Fig. 5D.1: NMR photoswitching of **1g**: (a) reverse switching, (b) forward switching.

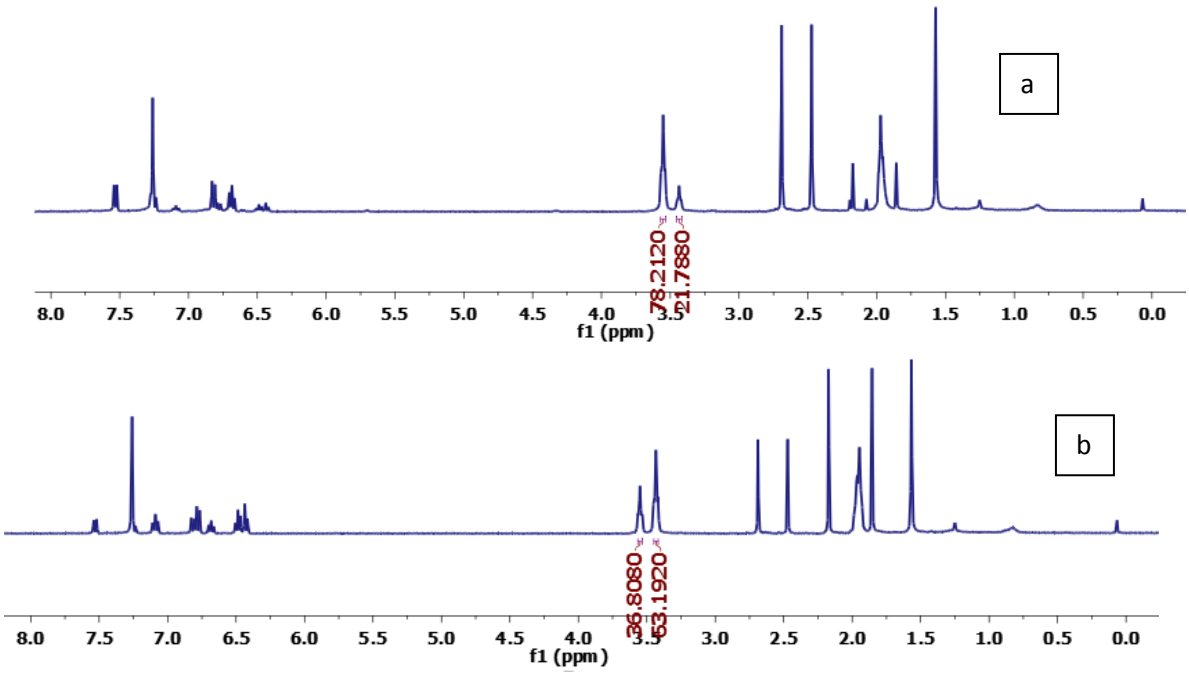

Fig. 5D.2: NMR photoswitching of **1a**: (a) reverse switching, (b) forward switching

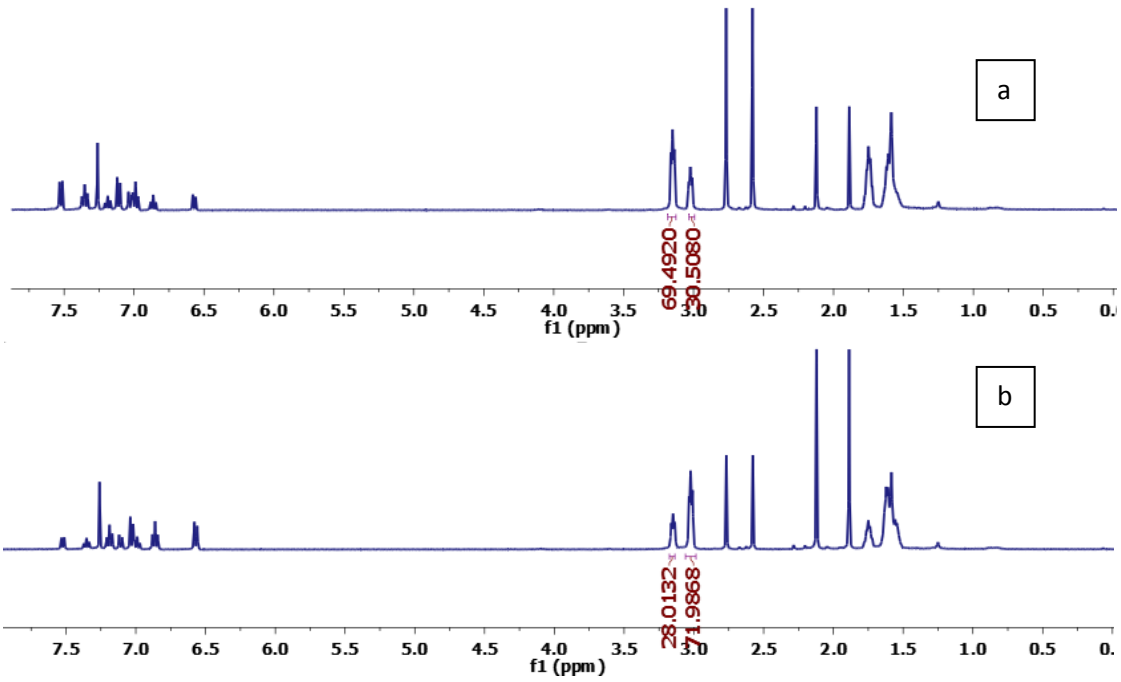

Fig. 5D.3: NMR photoswitching of **1b**: (a) reverse switching, (b) forward switching

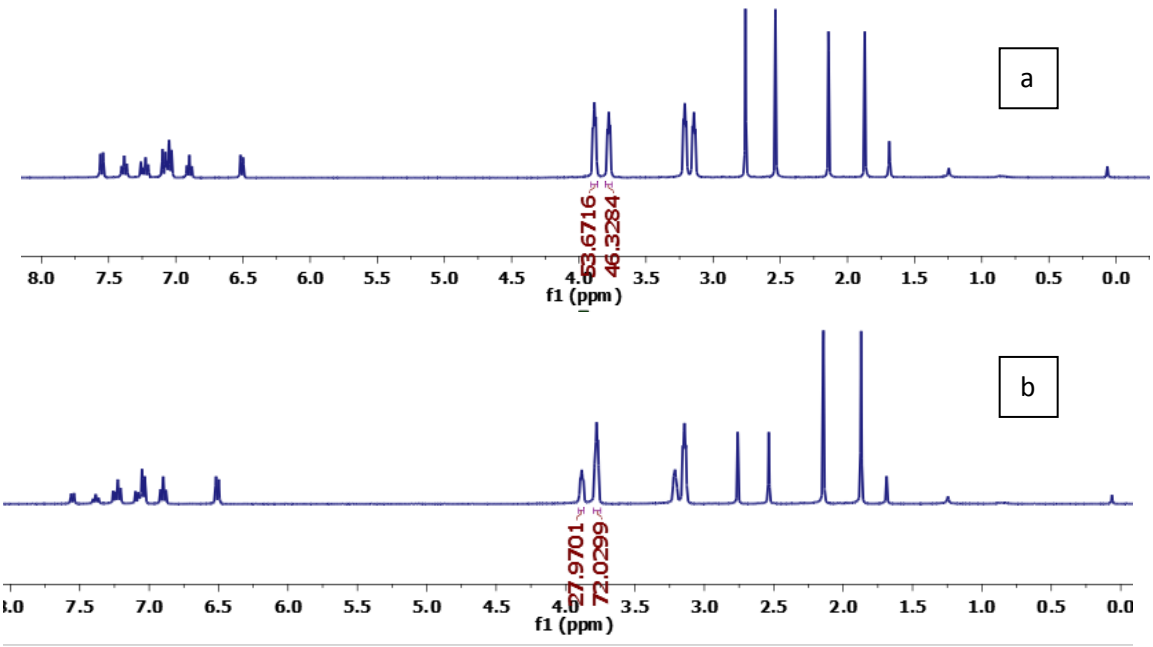

Fig. 5D.4: NMR photoswitching of **1d**: (a) reverse switching, (b) forward switching

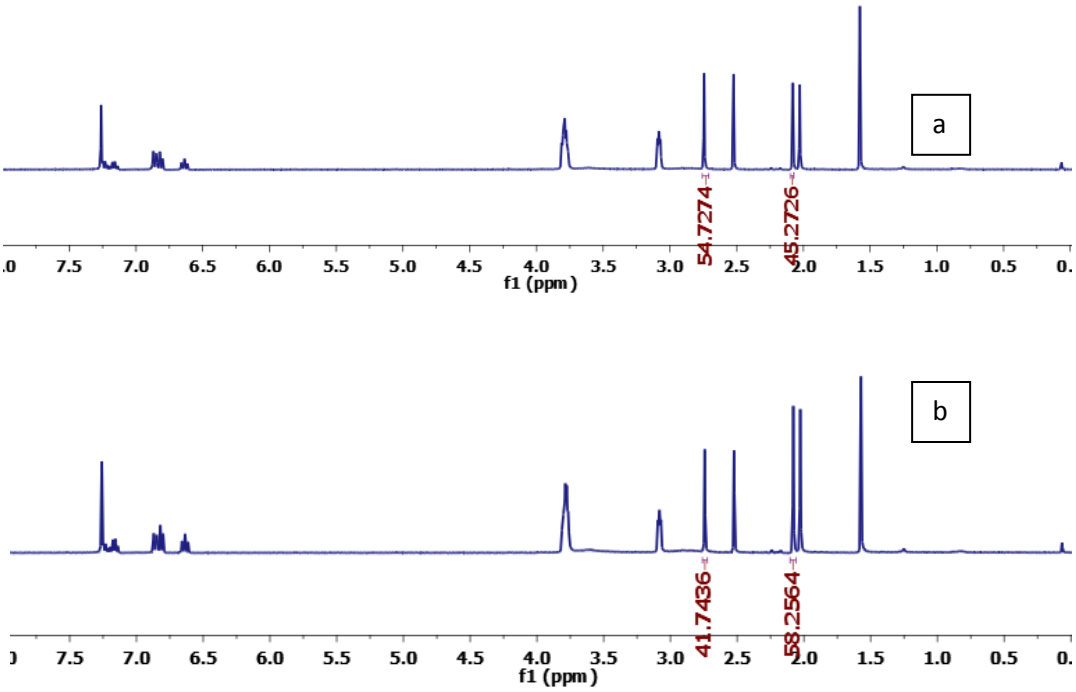

Fig. 5D.5: NMR photoswitching of **1i**: (a) reverse switching, (b) forward switching

Irin P Tom

Curriculum Vitae

IISER Mohali
Sector 81, Manauli P.O, Punjab
India
(+91) 8606933570
irinptom999@gmail.com
D.O.B.:17/08/1996

Education

2014-Present **Integrated BS-MS Chemistry**, *Indian Institute of Science Education and Research (IISER), Mohali*.
MS Research (pursuing): Azoheteroarene Based Visible Light Photoswitches
CPI: 8.7 (at the end of 9 out of 10 semesters)

2012-2014 **Higher Secondary Education**, *St. George Higher Secondary School*, Aruvithura, *Kottayam*.
Grade: straight A+'s, Certificate of Merit, for best academic performance in the School

2012 **Class 10**, *Little Flower High School*, Chemmalamattom, *Kottayam*.
Grade: straight A+'s, Certificate of Merit, for best academic performance in the School

Fellowships and Awards

2014-2019 INSPIRE Fellowship, a flagship program of Department of Science and Technology India, awarded to students who are placed in the top 1 percentage in their respective boards, in the Class 12 examination, to motivate them in the pursuit of research

2014-2019 Fellowship funded by the Department of Science and Technology, Government of India for doing summer internship

2016-2017 Certificate of merit, for the best academic performance in the second semester of 2016–2017 academic session

Summer Internships

May-July 2015 **Advanced Molecular Materials Research Centre**, *Mahatma Gandhi University*, *Kottayam*.
Performed under the guidance of Prof. Suresh Mathew
Topic: Computational design of Anthanthrene derivatives for Solar cell and OLED applications

May-July 2016 **National Institute for Interdisciplinary Science and Technology(CSIR-NIIST)**, *Thiruvananthapuram*.
Performed under the guidance of Dr. Narayanan Unni K.N.
Topic: Fabrication and Characterisation of Organic Photovoltaic Devices

May-July 2017 **Indian Institute of Science Education and Research**, *Mohali*.
Performed under the guidance of Dr. Santanu Kumar Pal
Topic: Preparation of Liquid Crystal based Biosensors

May-July 2018 **Indian Institute of Science Education and Research**, *Mohali*.
Performed under the guidance of Dr. Sugumar Venkataramani

Topic: Synthesis and Photoswitching studies of Multiple Azoarene Connected Systems

Research Interests

Physical Chemistry

Analytical Chemistry

Skills and Background Knowledge

Software packages: Gaussian09, ChemDraw, MestReNova, Origin 8.5

Experimental techniques: UV-Vis Spectroscopy, Fluorescence Spectroscopy, FTIR Spectroscopy, NMR Spectroscopy, Separation and Purification techniques

Teaching Experience

Teaching Assistant in Spectroscopy and Organic Chemistry laboratory courses

Conference

Frontiers in Chemical Sciences (FICS - 2018), IIT Guwahati

Recent Advances in Organic and Bio-organic Chemistry (RAOBC - 2019), IISER Mohali

Languages

English: Good oral and written skills

Malayalam: Good oral and written skills

Extracurricular activities and Hobbies

Volunteered for cultural and departmental activities

Painting

References

- Dr. Sugumar Venkataramani, Assistant Professor, Chemical Sciences

Address: IISER Mohali, Knowledge City, Sector 81, Manauli PO, SAS Nagar, Punjab, India, 140306

Email: sugumarv@iisermohali.ac.in

- Dr. Narayanan Unni K N, Principal Scientist and Head, Photosciences

Address: CSIR – National Institute for Interdisciplinary Science and Technology (NIIST) Industrial Estate PO, Thiruvananthapuram, Kerala 695019

Email: unni@niist.res.in